CCVJ'S FLUORESCENCE LIFETIME AS A VISCOSITY MEASUREMENT TOOL AND ITS POSSIBLE APPLICATION AS A TUNABLE PICOSECONDS REFERENCE LIFETIME STANDARD

A Thesis presented to

the Faculty of the Graduate School

at the University of Missouri-Columbia

In Partial Fulfillment

of the Requirements for the Degree

Master of Science

---

by

SASSON HAVIV

Dr. Mark A. Haidekker, Thesis Supervisor

DECEMBER 2007

The undersigned, appointed by the Dean of the Graduate School,

have examined the thesis entitled

CCVJ'S FLUORESCENCE LIFETIME AS A VISCOSITY MEASUREMENT TOOL AND ITS POSSIBLE APPLICATION AS A TUNABLE PICOSECONDS REFERENCE LIFETIME STANDARD

presented by Sasson Haviv,

a candidate for the degree of Master of Science,

and hereby certify that, in their opinion, it is worthy of acceptance.

_____

Dr. Mark A. Haidekker, Department of Biological Engineering

_____

Dr. Sheila A. Grant, Department of Biological Engineering

_____

Dr. Gerald A. Meininger, Department of Pharmacology and Physiology

ACKNOWLEDGEMENTS

I would like to thank Dr. Mark Haidekker for supporting this project and Darcy Lichlyter for her help in the lab. I also extend great thanks to Laura Valverde and Ali Shuaib for their support and help during this project. Finally, I would like to thank my parents, Batia and Saul Haviv, and my brothers and sister, Yehuda, Ilan and Merav, for their continuous support over the years.

.

TABLE OF CONTENTS

LIST OF ILLUSTRATIONS

Figure Page

LIST OF TABLES

CHAPTER 1

Viscosity

1.1 Introduction

Viscosity of a fluid is defined as the fluid's resistance to shear. Viscosity, η, is defined as the ratio between the fluid shear stress to the shear rate. Newton found that if a fluid is contained between two parallel plates, where the bottom plate is static while the upper plate spins with velocity Vo, the velocity profile of the fluid increases linearly from 0 (at the bottom of the plate) to Vo at the upper plate (Figure 1). The velocity gradient which is also called the shear rate equals to the change of velocity over the change of distance.

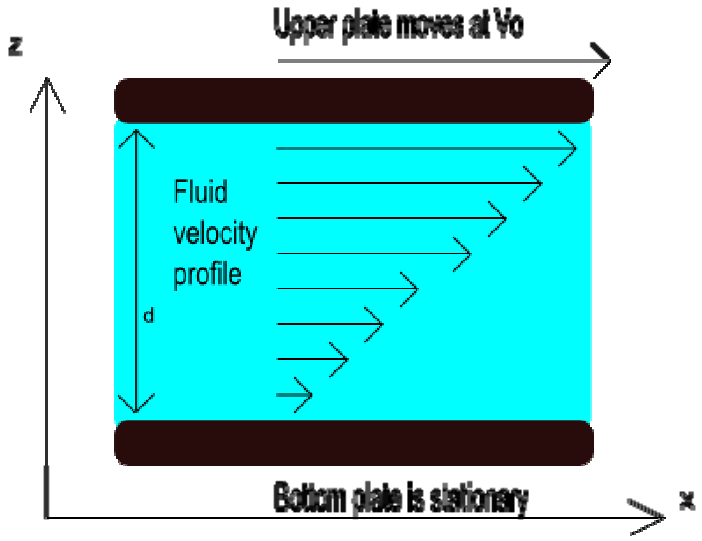

Figure 1: Velocity profile of fluid contained between a stationary and moving parallel plates.

$$D = \frac{dV}{dy} \tag{1}$$

Where D is the shear rate, dV is the change of velocity and dy is the change of distance. Since different fluid layers move at different speeds neighboring layers will develop frictional forces. This is referred to as shear stress. Newton's law of viscosity states that the shear stress is proportional to the sharing rate.

$$\tau = \eta D \tag{2}$$

Where τ is the shear stress and η is the viscosity. The unit of τ is force per unit area (N/m^2) which is represented by [Pa]. The shear rate unit is ((m/s)/m) which is simplified to [s^{-1}]. Thus, by rearranging Equation 2,

$$\eta = \frac{\tau}{D} \tag{3}$$

the unit of viscosity will be [Pa*s]. When dealing with fluids the unit of viscosity is usually given as [mPa*s] due to the low viscosities of fluids.

On a molecular level, the fluid's viscosity is determined by the interaction between the molecules. The friction that occurs between neighboring fluid layers is a consequence of the molecules bumping into each other and generating frictional force as well as heat. The forces that are involved in the intermolecular

interactions are: Van Der Waal's forces, charge, and dielectric effects where a stronger interaction causes a higher frictional force and higher viscosity. These forces are distance dependent and are inversely proportional to the free volume between the molecules. Consequently, free volume is inversely proportional to viscosity. Molecule size plays an important factor in free volume determination. Doolittle studied the effect of molecular weight of paraffin on viscosity under constant temperature. He established a mathematical relationship that describes liquid viscosity as a function of free volume (Doolittle 1952).

$$\eta = Ae^{\frac{Vo}{Vf}} \tag{4}$$

Where A is a constant, Vo is the van der Waals volume and Vf is the free volume of the solvent. The viscosity dependency on free volume gives an alternative approach to the measurement of viscosity and even allows for microviscosities determination. However, the commercial viscometers that are available in the market don't use the free volume principle but are based on finding the ratio of shear stress to shear rate.

1.2 Commercially available viscometers

1.2.1 Cone and plate viscometer

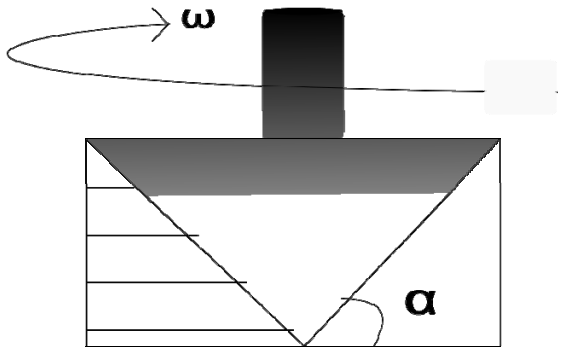

Figure 2: Schematic of cone and plate viscometer.

The cone and plate viscometer is made of a flat stationary plate and a rotating cone. The fluid is placed between the plate and the rotating cone and the torque on the spindle is measured. The device geometry causes uniform shear rate distribution which reduces measurement errors.

For the viscosity calculation (Equation 5) the torque, angular velocity, cone's radius, and the cone's angle are needed.

$$\eta = 3T\alpha / \left(2\pi R^3 \omega\right) \tag{5}$$

Where η is viscosity, α is the angle of the cone with respect to the plate, ω is the angular velocity, R is the cone's radius, and T is the torque on the spindle and is

related to the surface area of the cone. This cone-and-plate viscometer belongs to a group of rotational viscometers that have a disadvantage that several kinds of cones are needed to cover a large range of viscosity. Hence, if we are interested in measuring the viscosity of a cooling fluid a continuous measurement is not possible.

1.2.2 Concentric-cylinder viscometer

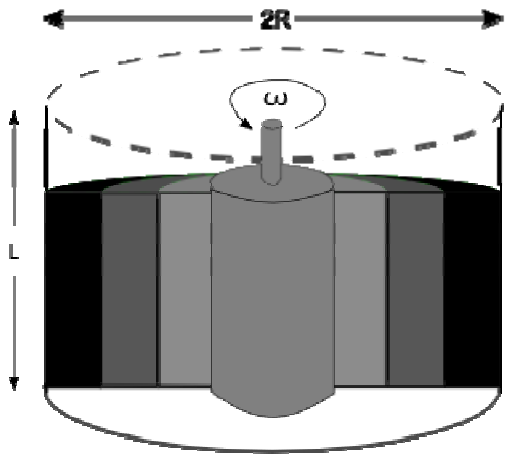

Figure 3: Schematic of concentric cylinder.

This viscometer also belongs to the group of rotational viscometers however; the geometry of the device gives it certain advantages. The fluid is sandwiches between a rotating inner cylinder and a static outer cylinder. The torque on the spindle is measured and used to calculate the viscosity (Equation 6).

$$\eta = \frac{T(k-1)}{2\pi R^2 L k^3 \omega} \tag{6}$$

Where T is the torque, and ω is the angular velocity. The large contact area of the inner cylinder allows for accurate measurements of low viscosity fluids.

1.2.3 Capillary viscometer

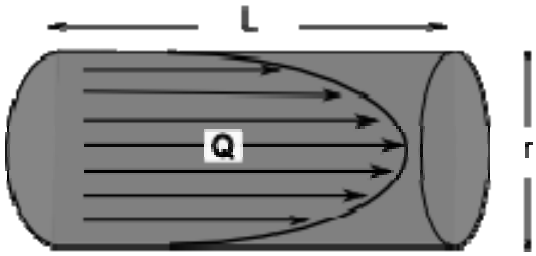

Figure 4: Schematic of capillary viscometer.

In capillary viscometers the flow rate and the pressure difference between the two ends of the capillary are used to calculate viscosity.

$$\eta = \frac{\Delta P \pi r^4}{8LQ} \tag{7}$$

Where ΔP is the pressure difference between the exit and entrance of the capillary, and Q is the flow rate. Capillary viscometers call for large sample volume for accurate measurements (Reinhart and others 1984) and the fluid requires high shear rates (McGrath and Penny 1976). The drawbacks of all mechanical viscometers are: long measurement time (several minutes in most cases), large sample size, time consuming cleaning procedures between

measurements, and possible errors arising from protein linkage to surfaces (Cokelet 1972).

But what is the significance of viscosity in real-world applications? Many industries are interested in knowing the viscosity of the fluids they manufacture or work with. The measured viscosity is used to design the pipes used for the fluid's transportation (e.g. in the oil industry) and a better control of the fluid's viscosity can also reduce the transportation cost. In the medical field, the viscosity of blood and blood plasma and their connection to health related conditions is gaining importance. As will be summarized in the next section.

1.3 Viscosity of blood plasma

Blood plasma viscosity irregularities are associated with various ailments such as diabetes (Kumari and others 2005; McMillan 1982), hypertension (Letcher and others 1981), infraction (Harkness 1971), increased blood pressure (Cinar and others 2001) , systemic lupus erythematosus (Rosenson and others 2001), and infection (Harkness 1971; Yudkin and others 2000). Most of the diseases associated with blood plasma anomalies cause an alteration in the protein levels (Harkness 1971). Protein–induced hyper-viscosity was linked to increased risk of atherosclerosis (Harkness 1971; McGrath and Penny 1976; Wells 1970; Yudkin and others 2000). Furthermore, smoking was found to increase blood plasma viscosity (Otto and others 2001) which helps link cigarette consumption and increased risk of heart disease. Changes in blood plasma viscosities are also linked to aging (Roe and Harkness 1975), extended bed rest (Kaperonis and others 1988), and pregnancy (Heilmann 1986). It has been

proposed that blood plasma viscosity can be used as a diagnostic tool for the early detection of diseases (Harkness 1971). Blood plasma viscosity also plays an important role in transfusion medicine and must be monitored during transfusions and plasmpheresis (McGrath and Penny 1976). The Harkness capillary viscometer, a specialized viscometer for the measurement of blood plasma viscosity, is suggested by the International Committee for Standardization in Hematology (Anonymous 1984). The Harkness capillary viscometer can measure sample sizes of 0.5 ml in less than a minute. However, cleaning between measurements increases the measurement time, and in order to obtain reliable results the air/solution interfaces effects must be accounted for or controlled (Cokelet 1972). These impediments reduce the effectiveness of the Harkness viscometer in clinical settings.

Molecular rotors are fluorescent viscosity probes that use the free space approach to determine viscosity. This new approach that uses a non- mechanical mechanism for viscosity measurement may help physicians attain a faster result. The molecular rotor allows not only for continuous viscosity measurements but also provides the ability to determine micro-viscosities (which is not possible when using mechanical devices).

CHAPTER 2

Fluorescence

2.1 What is fluorescence?

Fluorescence is a popular method that is used in sensors for medical applications, DNA sequencing, cellular and molecular imaging, toxin detection, and many more other applications (Badugu and others 2005; Carreon and others 2007; Jamieson and others 2007; Lei and others 2004; Rowe-Taitt and others 2000; Zhu and others 2004). The widespread use of fluorescence is due to the high sensitivity the method offers, the growth in availability of fluorescent probes and to the reduced price of steady state and time domain instrumentation.

The phenomenon of fluorescence is the emission of a photon from a molecule in the excited state. For a molecule to be in an excited state one of the electrons must "jump" to a higher energy level. This jump occurs as a consequence of a photon being absorbed by the molecule. The excited state lasts for a short time (usually on the nanosecond scale) and a return to the ground state occurs through either a photon emission (radiative decay) or a non radiative decay (for example: thermal relaxation).

The energy levels that the electron "jumps" to are described by atomic orbitals. The Heisenberg uncertainty principle states that we can not define the momentum and position of an electron at the same time so it is impossible to know the current and subsequent location of the electron. However, by mapping only the locations of the electron at different points of time a three dimensional shape surrounding the nucleus is obtained. This shape is represented by an

atomic orbital and is really a probability density for the electron's location. An electron can exist only in a distinct energy level and so it cannot occupy two different orbitals at the same time. There are many orbitals surrounding the nucleus and each one is given a principal quantum number(n) and an angular momentum quantum number (l) corresponding to the orbital's energy level. The further the orbital is from the nucleus the higher its energy level. Orbitals are organized into shells and subshells. A shell consists of orbitals that have the same principal quantum number (n=1, 2, 3, 4.) and can hold up to 2n^2 electrons. The subshells are divided according to the angular momentum quantum number (l=0, 1, 2...n−1) and can hold up to 2l+1 electron pairs. An atom in its ground state will have all its electrons in the lowest energy configuration possible. When two atom's orbitals overlap two types of covalent bonds may occur: σ and π bonds. The σ bond occurs when there is a complete overlap of the orbitals and the orbital overlap is along the internuclear axis. The π bond occurs when there is only partial overlap of the orbitals and the bond form from sideways overlap of orbitals (Figure 5).

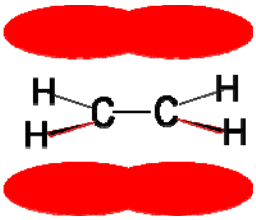

Figure 5: π bond.

In aromatic compounds the π bonds can interact with each other and form a very stable structure through resonance.

Figure 6: Delocalization of π electrons in the benzene ring.

The six π electrons in the benzene ring are delocalized and are equally shared between all six carbon atoms (Figure 6). In the case of benzene, there are three bonding π orbitals and three anti-bonding π* orbitals.

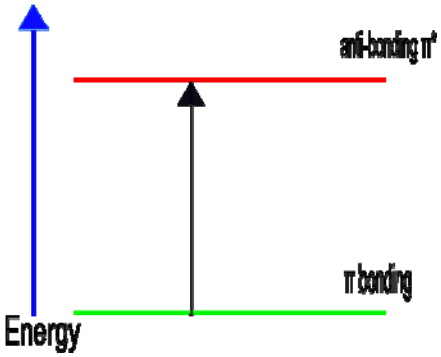

Figure 7: π* Orbital gets populated from the highest occupied molecular orbital subsequent to photon absorption.

The anti-bonding π* orbitals cause repulsion rather than attraction between participating nuclei, and are of higher energy level (less stable) than the bonding π orbitals (Figure 7). These anti-bonding π* orbitals stay vacant at the ground state.

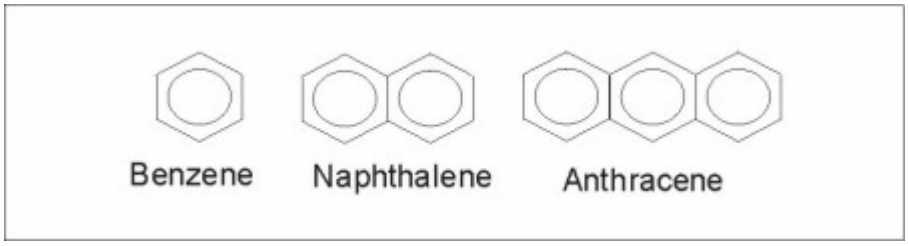

Figure 8: Increasing delocalization of π electrons increases the absorbed photon's wavelength (lower energy). Excitation wavelengths of: Benzene=240nm, Naphthalene =290nm, Anthracene =365nm.

In aromatic compounds (when excited by UV or visible light) it is usually the π electron that jumps to the π* anti-bonding orbital (the σ electron requires a higher energy photon in order to jump to the anti-bonding σ* orbital). The amount of delocalization of the π electrons directly relates to the energy input needed for the electron to cross the gap. Higher level of delocalization reduces the gap between the π bonding and the π* anti-bonding orbital and a lower energy photon (higher wavelength) is needed to cross the gap (Figure 8). When a photon of certain energy is absorbed by a fluorophore, an electron from the π bonding orbital or an unbound electron moves to occupy the anti-bonding π* orbital. The photon's energy depends upon its wavelength (Equation 8).

$$E = \frac{hc}{\lambda} \tag{8}$$

Where h is Planck's constant (h=6.625x10-34 Js), c is the speed of light in a vacuum, and λ is the wavelength. It is important to note that each fluorophore responds only to certain range of wavelengths and not to all wavelengths. For each fluorophore, specific photon energy is needed to be absorbed in order for the electron to cross the gap between the π electron and the anti-bonding π* orbital.

Jablonski proposed a diagram that explains the processes that are involved with light absorption by fluorophores.

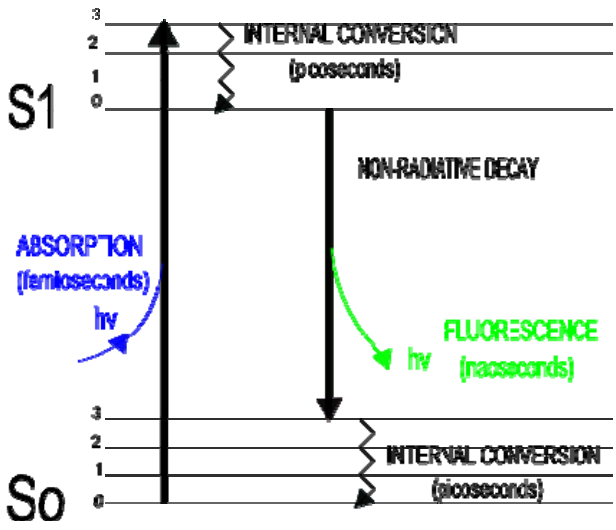

Figure 9: Simplified Jablonski diagram.

In the simplified Jablonski diagram (Figure 9) we observe the S_0, and S_1 (S_2 is not shown since a photon with wavelength less than 200nm is needed to populate this energy level) energy levels corresponding to the ground state and

excited state respectively. Both these states have several vibrational energy levels described by 0, 1, 2, etc. Absorption is shown by a vertical arrow from S_0 (ground state) to the higher vibrational energy levels of S_1 (excited state). Absorption is a very fast process on the femtoseconds timescale. Internal conversion (Picoseconds timescale) occurs immediately and the electron reaches the lower energy level of S_1 where it usually stays for several nanoseconds. From the excited state there are several competing pathways for the electron to return to ground state. Nonradiative decay pathways include a return to the ground state through resonance energy transfer, heat dissipation, and molecular rearrangement (intersystem crossing is not shown since it is not relevant to this research and can be neglected). An alternative pathway is a return to ground state through photon emission (fluorescence). Sir G. G. Stoke observed that the photon being emitted is of lower energy than the absorbed one. The difference between the emission wavelength and the excitation wavelength is called Stokes shift and the emitted photon is said to be red shifted. This accounts for the energy loss through internal conversion both in the S_1 and S_0 energy levels.

Another interesting phenomenon related to photon emission is the Franck-Condon principle. It states that electronic transitions are most likely to occur without molecular changes (that is why absorption and emission are represented by vertical lines in the Jablonski diagram). As a result, the shape of the emission spectra of a fluorophore is usually independent of excitation wavelength. However, the intensity is dependent on the excitation wavelength.

2.2 Quantum yield and lifetime

The most important characteristics of a fluorophore are: excitation and emission wavelengths, quantum yield, and the fluorescence lifetime. Excitation and emission wavelengths are important when considering applications. Quantum yield is the ratio of emitted photons and absorbed photons.

$$Q = \frac{Kr}{Kr + Knr} \tag{9}$$

Where Q is the quantum yield, Kr is the radiative decay, and Knr is the sum of all nonradiative decay pathways. The quantum yield varies not only between different fluorophores but also for the same fluorophore in different environments. The quantum yield of Rhodamine in ethanol which is one of the brightest fluorophores is 0.95, but when Rhodamine is dissolved in water the quantum yield decreases to 0.90 (Douglas and others 2002). When determining oxygen levels through the skin, the fluorophores utilized are usually excited by light with 600nm or higher wavelengths in order to avoid absorbance and scattering effects (Bambot and others 1995). A high quantum yield is recommended for easier detection (stronger signal) and it is necessary for the fluorophores to dissolve in the observed environment.

Fluorescence lifetime is the average time that an electron spends in the excited state prior to returning to ground state (Lakowicz 2006). The fluorescence life time is given by:

$$\tau = \frac{1}{Kr + Knr} \tag{10}$$

Where τ is the fluorescence lifetime.

Fluorescence is a random process that can be described by an exponential decay model.

.

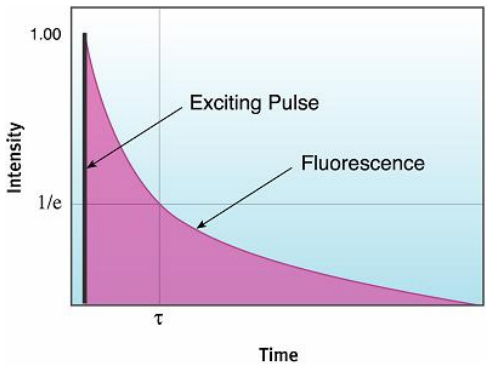

Figure 10: Excitation pulse followed by a single exponential decay. The fluorescence lifetime τ equals 1/e (ISS 2007).

$$I(t) = I_0 e^{\frac{-t}{\tau}} \tag{11}$$

where I_o is the intensity at t=0. Some fluorophores exhibit only a single exponential decay while others exhibit a multi-exponential decay behavior which is described by Equation 12.

$$I(t) = \sum_i \alpha_i e^{\frac{-t}{\tau_i}} \tag{12}$$

Where α_i is the pre-exponential factor.

Multi-exponential decay behavior may occur because of environmental factors such as quenching, energy transfer processes (these processes are described in the next section), or due to inhomogeneous environments.

Fluorescence lifetime in the absence of nonradiative decay is called natural lifetime, τ_n, and is given by:

$$\tau_n = \frac{1}{Kr} \tag{13}$$

Natural lifetime can be attained only in the absence of quenchers and at very low temperatures where nonradiative decay due to molecular vibrations is completely brought to a halt. By combining Equations 10 and 11 the quantum yield can be calculated from the fluorescence and natural lifetime.

$$Q = \frac{\tau}{\tau_n} \tag{14}$$

2.3 Quenching

Processes that result in reduced fluorescence intensity are termed quenching processes (Lakowicz 2006). Some of these processes are dynamic and static quenching, and molecular rearrangements. Dynamic quenching, also called collisional quenching, occurs when a quencher collides with a fluorophore that is in the excited state (during the fluorophore‘s lifetime). As a result, the fluorophore returns to the ground state without photon emission. Molecular oxygen, aromatic and aliphatic amines, iodide, bromide, and purines are only a few substances that act as quenchers. There are several quenching mechanisms such as: intersystem crossing to triplet state, formation of an excited charge transfer complex, and donation of electron from fluorophore to quencher. Collisional quenching is expressed by the Stern-Volmer Equation (15).

$$\frac{F_0}{F} = 1 + K|Q| = 1 + k_q \tau_0 |Q| \tag{15}$$

Where F_0 is the unquenched fluorescence intensity, F is the quenched fluorescence intensity, K is the Stern-Volmer quenching constant, k_q is the

bimolecular quenching constant, τ_o is the unquenched lifetime, and [Q] is the quencher concentration.

In Static quenching a non-fluorescent ground state complex is formed between the fluorophore and the quencher (Lakowicz 2006). Static quenching is described by Equation 16,

$$\frac{F_0}{F} = 1 + K_S[Q] \tag{16}$$

Where K_S is the association constant for complex formation, and [Q] is the concentration of the quencher. Both static and dynamic quenching lead to lower intensity however, only dynamic quenching leads to reduced fluorescence lifetime. In the case of static quenching, the fluorescence lifetime is unchanged since only the non-complexed fluorophores are able to participate in emission and their average lifetime is still the same as any excited fluorophore population. An additional quenching process is resonance energy transfer (RET). The main distinction between RET and collisional and dynamic interaction is that RET doesn't require molecular contact. In RET the excited fluorophore acts as a donor and transfers energy to a fluorescent or non-fluorescent molecule that acts as the acceptor. The donor's emission wavelength band overlaps the acceptor's absorption band; however the acceptor doesn't have to be fluorescent. If the acceptor is fluorescent, it may go back to the ground state through photon

emission otherwise; the transferred energy will dissipate as heat. RET is distance dependent and the efficiency of energy transfer is described by:

$$E = \frac{R_0^6}{R_0^6 + r^6} \tag{17}$$

Where E is the energy transfer efficiency, R_o is the Forster distance (a dye-dependent constant), and r is the distance between the donor and the acceptor. Quenching of fluorophores is a frequently used method to obtain information about the fluorophore‘s surrounding. In the case of RET distances between sites on macromolecules can be calculated from the energy transfer efficiency, dynamic quenching can be used to find out the fluorophores location on a macromolecules.

2.4 Fluorescent probes

Some fluorophores exhibit a noticeable sensitivity to environmental factors such as pH, viscosity, and charge. These sensitivities are accounTable to changes of fluorescence intensity and fluorescence lifetime. Thus, tracking fluorophores intensity or lifetime is utilized to probe specific properties of the environment. Several fluorophores and their applications are described to enhance the reader’s understanding of fluorescent probes.

Chloride is an important biological component vital to neuronal processes and cellular pH. A number of chloride sensitive probes have been developed (Geddes and others 2001; Huber and others 1999). In most cases, chloride acts as

a collisional quencher and reduces both intensity and fluorescence lifetime. Thus, the measured intensities or lifetimes can be used to determine chloride's concentration.

Prodan is a fluorescent molecule that exhibit solvent polarity fluorescence shifts. Prodan and Prodan derivatives are frequently used to probe the environment of cell membranes and help map the changes of phospholipids structures (Krasnowska and others 2001).

ANS is another useful fluorophore which is useful in protein labeling. In water its fluorescence lifetime and quantum yield are approaching zero however when bounded to proteins its nonpolar region is protected and both quantum yield and lifetime are greatly increased (Chakraborty and Basak 2007).

An energy transfer system is described to give a better appreciation of fluorescent sensor design. A non invasive glucose sensor designed by Tolosa utilizes energy transfer to determine glucose levels (Tolosa and others 1997). Concanavalin A was labeled by Ruthenium metal-ligand complex (RuCon) and acted as the donor. Upon bondage of the acceptor, insulin linked malachite green labeled with maltose (MIMG), to the donor (RuCon) a decrease in intensity and fluorescence lifetime of the donor occurred. Competitive displacement of the acceptor by glucose led to an increase in intensity and fluorescence lifetime of RuCon which were used to determine glucose levels (Tolosa and others 1997).

DCVJ is fluorescent molecule that is viscosity dependent and belongs to the family of molecular rotors. Its quantum yield and fluorescence lifetime increase with increased viscosity. Haidekker (2001) used this phenomenon to

track the response of the cell's viscosity to fluid shear stress. Another member of the molecular rotor family, CCVJ, is the main focus of this research.

CHAPTER 3

Fluorescence Spectroscopy

3.1 Introduction

In general there are two types of fluorescence measurements: steady state and time resolved spectroscopy. Steady state uses a steady excitation source to continuously illuminate the fluorophore and detect the emission intensity. Since the fluorescence lifetime is in the picoseconds scale steady state is achieved almost instantly and the measurement is really an averaging of the time resolved intensity decays (Equation 17). Time resolved fluorescence uses an excitation source with a very short light pulse (much shorter than the fluorescence lifetime) and the detector measures intensity changes in the nanosecond timescale. The intensity decay was given before in Equation 11 repeated here.

$$I(t) = I_0 e^{\frac{-t}{\tau}} \tag{11}$$

where I_o is the intensity at t=0.

The steady state is given by:

$$Iss = \int_0^\infty I_0 e^{\frac{-t}{\tau}} dt = I_0 \tau \tag{18}$$

where Iss stands for steady state intensity.

There are certain advantages and disadvantages for steady state spectroscopy. The instrumentation is cheap and easy to operate, the results are easily interpreted and there are many years of research to turn to as reference. However, there are two major disadvantages: there is a loss of information due to the averaging process as well as mistakes arising from concentration inaccuracies and other optical properties (Lakowicz 2006). The loss of information can be easily illustrated by observing the emission of two different fluorophores with overlapping emission spectra. Steady state measurements cannot necessarily identify that two fluorophores exist in the solution. However, time resolved measurement of the same solution may confirm that there are two different decay times corresponding to the two different fluorophores provided that the lifetimes are sufficiently separated. Further more the contribution (percentage) of each fluorophore will be known.

Another big advantage of time resolved spectroscopy is that fluorescence lifetimes are typically independent of concentration (Lakowicz 2006). This helps in eliminating errors arising from pippeting mistakes as well as from changes the probe's concentration due to alterations the environment (cellular imaging). Even though time resolved spectroscopy instrumentation is expensive and requires a higher skill to operate, it does overcome the main problems associated with steady state spectroscopy.

Complicating factors in time resolved and steady state measurements

An unwanted quenching process that might be encountered is called "inner filter effect". Inner filter effect occurs when the fluorophore concentration is too high. As a result the excitation light distribution is inhomogeneous through the solution and only a small percentage reaches the fluorescent molecules that are observable by the detector. Inner filter effects leads to reduction of both intensity and fluorescence lifetime thus, analysis should include the possibility of inner filter effects.

3.2 Time and Frequency domain methods

The popular methods that are used in time resolved spectroscopy are the time and frequency domain techniques. In the time domain method the most common method is Time correlated single-photon counting (TCSPC). In this method a short light pulse is used to excite the sample (on the pico or femtosecond timescale). The first arriving photon is detected and "placed" in a bin corresponding to its arrival time. This process repeats itself many times and a photon arrival time distribution histogram is obtained. Once enough photons have been detected the histogram accurately represents the intensity decay and can be analyzed to determine the fluorescence lifetimes.

In the frequency domain method which is also called phase-modulation method the sample is excited by a frequency modulated light source and the frequency response of the sample is analyzed to determine the fluorescence lifetimes. The phase modulation method was used in this research and so an in

depth explanation of the method and the data analysis procedures involved are given.

3.3 The phase modulation method

As explained before, the sample is excited by intensity modulated light at varying frequencies. The sample absorbs the light however, the delay time (fluorescence lifetime) between absorption and emission causes phase shift between excitation and emission as well as amplitude reduction of the emission's intensity (Figure 11).

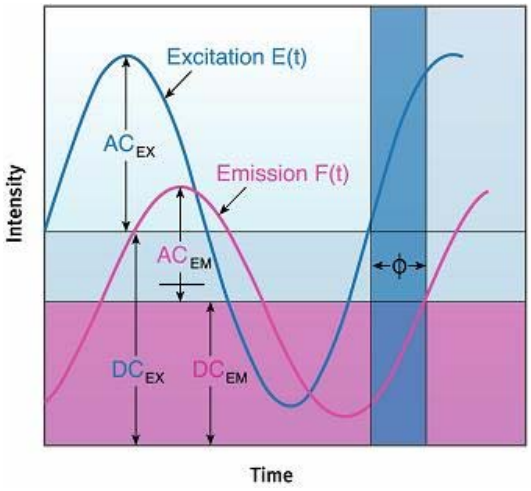

Figure 11: Example of phase shift and modulation of the emission wavelength (ISS 2007).

These changes are frequency dependent and as the modulation frequency is increased, a frequency response of the sample is obtained. The phase shift increases from 0 to 90 degrees while the intensity modulation decreases from 1 to

o (Figure 12). The modulation value is given as the ratio of the AC component and the DC component so that the relative modulation (m_ω) is given as:

$$m_\omega = \frac{\left[\frac{AC}{DC}\right]_{EMISSION}}{\left[\frac{AC}{DC}\right]_{EXCITATION}} \tag{19}$$

For a single exponential decay the fluorescence lifetime can be directly calculated from Equations 20 and 21.

$$\tan \phi_\omega = \omega\tau \tag{20}$$

$$m_\omega = \left(1 + \omega^2\tau^2\right)^{-\frac{1}{2}} \tag{21}$$

Where Φ_ω is the phase shift in radians and ω is the 2π times the modulation frequency in radians/s, and m_ω is the relative modulation at a given frequency.

For a single exponential decay, the phase and modulation lifetimes are equal and the fluorescence lifetime can be determined from only a few modulation frequencies. For a multi exponential decay the phase and modulation values represent a complex weighting of several variables, and the fluorescence lifetimes can be calculated only by measuring a wide range of modulation frequencies (will

be explained in detail in the next section) (Lakowicz 2006). Each fluorophore has its own characteristic frequency response.

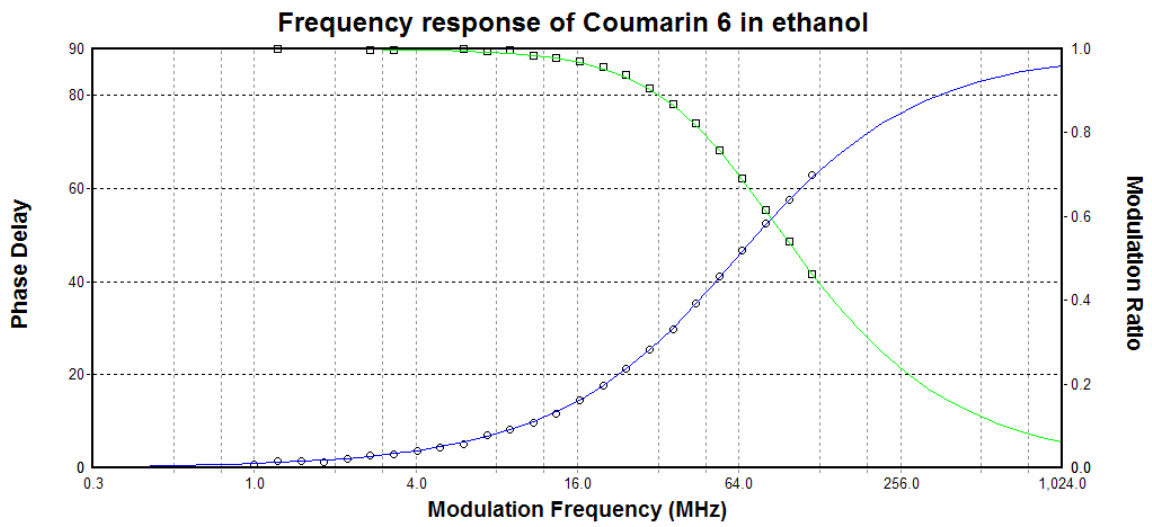

Figure 12: Frequency response of Coumarin 6 in ethanol.
τ=2.54 nanoseconds X^2=1.01

The frequency response shape depends on the number of decay times and their contribution. In the case of multi-exponential decay, each lifetime will have a certain contribution (percentage) to the weighted lifetime. The contribution of each decay (f_i) is given as:

$$f_i = \frac{\alpha_i \tau_i}{\sum_i \alpha_i \tau_i} \tag{22}$$

Where τ_i stands for fluorescence lifetime of each decay and α_i stands for the preexponential factor of each decay.

Thus, in a mixture of two fluorophores it is possible to determine the percentage of each fluorophore. In many cases a single fluorophore exhibits a multi-exponential decay where each decay time is due to certain effects of the environment (such as: viscosity, polarity, refractive index…). These "individual" decay times can be observed to monitor changes in the environment.

3.4 Frequency domain data analysis

The nonlinear least squares method is used to analyze the frequency domain data. The measured data is compared to a model (single or multi exponential decay) and the model's parameters are varied until the deviation from the measured data is minimized. The phase and modulation data can be analyzed individually or jointly. Sine and cosine transforms of the intensity data are used to predict the model (Equations 23, and 24)

$$N_{\omega} = \frac{\int_0^{\infty} I(t)\sin \omega t dt}{\int_0^{\infty} I(t)dt} \tag{23}$$

$$D_{\omega} = \frac{\int_0^{\infty} I(t)\cos \omega t dt}{\int_0^{\infty} I(t)dt} \tag{24}$$

Where I(t) stands for intensity as a function of time, ω is the circular modulation frequency and the denominator is used for normalization.

For a sum of exponentials as in the phase modulation method the transforms are:

$$N_\omega = \sum_i \frac{\alpha_i \omega \tau_i^{\,2}}{\left(1+\omega^2 \tau_i^{\,2}\right)} \Big/ \sum_i \alpha_i \tau_i \tag{25}$$

$$D_\omega = \sum_i \frac{\alpha_i \tau_i}{\left(1+\omega^2 \tau_i^{\,2}\right)} \Big/ \sum_i \alpha_i \tau_i \tag{26}$$

Where τ_i stands for fluorescence lifetime of each decay, α_i stands for the preexponential factor of each decay, ω is the circular modulation frequency and the denominator is used for normalization.

The pre-exponential factors α, and the lifetimes are varied to provide the smallest amount of deviation between measured and calculated data. The calculated phase and demodulation are given by:

$$\tan \phi_{C\omega} = \frac{N_\omega}{D_\omega} \tag{27}$$

and

$$m_{C\omega} = \left(N_\omega^{\,2} + D_\omega^{\,2}\right)^{\frac{1}{2}} \tag{28}$$

where $\Phi_{c\omega}$ and $m_{c\omega}$ stand for calculated phase shift and calculated modulation respectively. Finally, the measured and calculated values are used to provide the best model (lowest X_R^2 value).

$$X_R^2 = \frac{1}{v}\sum_{\omega}\left[\frac{\phi_\omega - \phi_{c\omega}}{\delta\phi}\right]^2 + \frac{1}{v}\sum_{\omega}\left[\frac{m_\omega - m_{c\omega}}{\delta m}\right]^2 \qquad (29)$$

Where $\delta\Phi$ and δm represent the uncertainties in phase and modulation values and v is the number of degrees of freedom. $\delta\Phi$ and δm are typically given the values of 0.2^o and 0.005 respectively (Lakowicz 2006). The quality of the fit is determined by the X_R^2 value where a value of unity indicates a perfect fit. A lower value than one will indicate that the uncertainties are overestimated. In order to reject the model one must consult a X_R^2 distribution Table. One will start analyzing the data using a single exponential decay and then increase the number of decays in order to reduce the X_R^2 value. In principle, an additional exponential decay parameter is accepted if the X_R^2 value is decreased by half or more (Lakowicz 2006).

CHAPTER 4

Frequency Domain Instrumentation

4.1 Overview

The first frequency domain device was used by Gaviola (1926) and measured the phase shift at a single fixed frequency. Gaviola's device was limited to measuring only single exponential lifetimes or mean lifetimes (in the case of multi-exponential decay). Later designs were able to use three fixed frequencies and so gain more information. However, the amount of information was still not sufficient to determine anything but mean lifetimes (for a single exponential lifetime the mean lifetime is the fluorescence lifetime). A big breakthrough was achieved when electrooptic modulators were used to modulate the excitation light (Lakowicz 2006). The electrooptic modulator is capable to modulate the signal in variable frequencies up to 200MHz and allowed for determination of multi exponential decay lifetimes. The signal readout was made easy by utilizing the cross correlation method. Cross correlation involves mixing of excitation and emission signals and to obtain a signal with low frequency. The method allowed for simplified electronics for the measurement of phase shift and modulation. Currently, 1GHz frequency domain commercial devices are available. They use pulsed laser diodes as an excitation light source and a multi-channel plate detectors for signal detection (Lakowicz 2006).

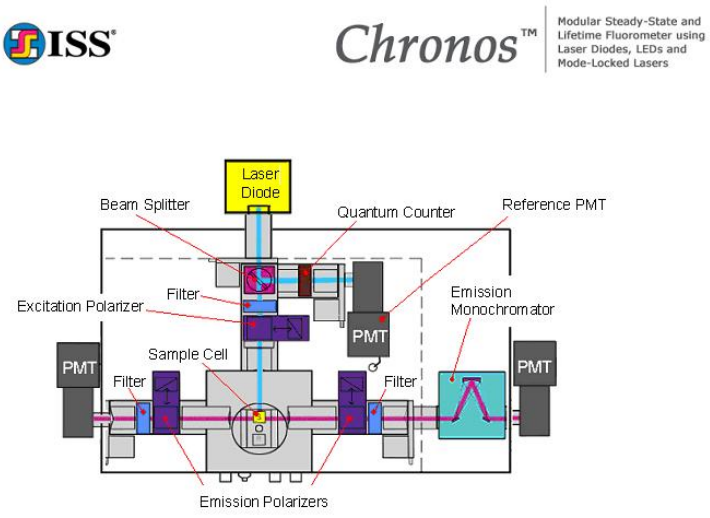

Figure 13: Schematic of the frequency domain spectrometer used in this research (ISS 2007).

4.2 Light sources

In the frequency domain method the excitation light source must be intensity modulated at different frequencies. There are two approaches that yield the desired outcome: usage of light modulators or using a light source that can be intrinsically modulated.

The electrooptic modulator uses two polarizers and a modulator made of a material that rotates polarized light when exposed to an electrical field (kaminov 1984). The applied voltage that causes the electrical field is proportional to the light intensity so by changing the voltage the light is intensity modulated usually following a sine wave. The frequency of the intensity modulated light is twice the frequency of the electric field. So by varying the frequency of the electric field, the light can be modulated at varying frequencies.

One drawback of light modulators is that they are limited to a frequency of 200MHz. This frequency is acceptable for measurement of multi exponential decays with nanosecond fluorescence lifetime. However, a higher frequency is required when trying to determine a picosecond lifetime, especially when trying to resolve a multi-exponential decay. Another shortcoming is that the light is attenuated to about 10% of the original intensity (Lakowicz 2006). Pulsed lasers, particularly laser diodes, are intrinsically modulated light sources (Lakowicz 2006). The harmonic frequency content of the laser is used for excitation at different frequencies. For example, a 5 ps pulse width with a repetition of 4 MHz can be used to excite samples at 4, 8, 12, 16, 20,... MHz all the way to GHz frequencies. The availability of laser diodes has dramatically reduced the cost of frequency domain devices.

LED's can help reduce the price even further. Led's can be modulated up to several hundreds MHz and are available at many wavelengths (Fantini and others 1994; Zukauskas and others). Szmacinski and Chang (2000) were able to measure the fluorescence lifetime of potassium bound and unbound CD 222 using 373nm LED as an excitation source. The free CD 222 fluorescence lifetime was found to be 0.15ns while potassium bound probe lifetime was0.67ns.

4.3 Cross correlation

Extracting the phase and modulation data from the output signal involves using the cross correlation method. In this method the gain of the detector is modulated at an offset frequency (Δf) from the frequency of the excitation light (F). The excitation and emission signals are mixed and result in a low frequency

signal (Δf) that contains both the phase and modulation data (Spencer RD and Weber G 1969). This low frequency signal is not only easy to analyze but also eliminates harmonics and other noise sources (Lakowicz 2006). A mathematical description of the cross correlation method adopted from Lakowicz (2006) is given below.

The high frequency time dependent intensity signal is given by Equation 30.

$$I(t) = I_o\left[1 + m\cos\left(\omega t - \varphi\right)\right] \tag{30}$$

The emitted high frequency signal is multiplied by the sinusoidal gain modulation (G(t)) of the PMT.

$$G(t) = G_o\left[1 + m_c\cos(\omega_c t + \phi_c)\right] \tag{31}$$

Where Go is the average value of the function and m_c, ω_c, and Φ_c are the modulation, frequency and phase of the cross-correlation signal. By multiplying Equations 30 and 31 and using trigonometric Equation for simplification Equation 32 is obtained.

$$S(t) = N_o G_o\left[\begin{array}{l} 1 + m\cos(\omega t + \phi) + m_c\cos\left(\omega_c t + \phi_c\right) + \\ \dfrac{m m_c}{2}\left(\cos\left(\Delta\omega t + \Delta\phi\right) + \cos\left(\omega_c t + \omega t + \Delta\varphi\right)\right) \end{array}\right] \tag{32}$$

Where $\Delta\omega=\omega_c-\omega$, $\Delta\Phi=\Phi_c-\Phi$.

The low frequency $\Delta\omega$ term can be isolated by using a low-pass filter. Since the low frequency $\Delta\omega$ contains the phase and modulation data, it simplifies the data extraction process.

4.4 Detection

In order to analyze the emitted light for phase shift and modulation data it must be converted to an easily analyzed signal. Photo multiplier tubes (PMTs), commonly used as detectors in frequency domain devices, by converting incoming photons to a measurable current. PMTs consist of a photocathode and series of dynodes (Figure 14).

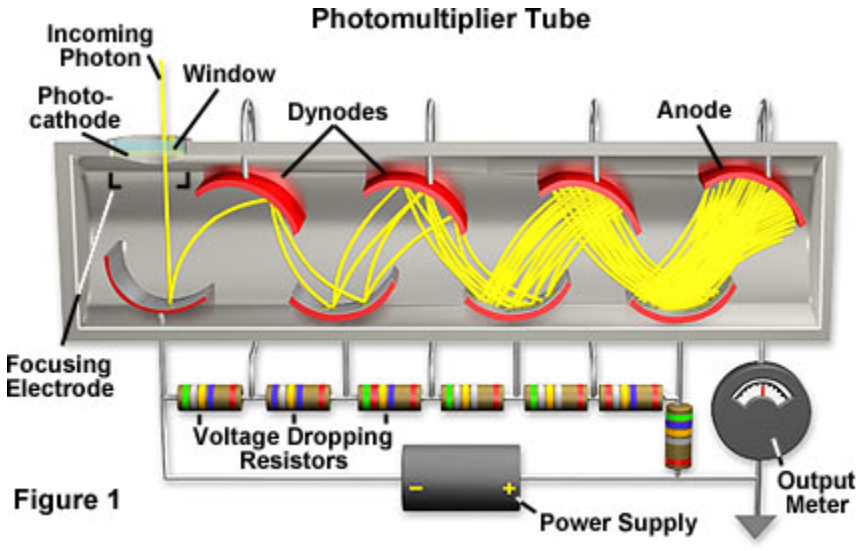

Figure 14: Image of a PMT (Molecular Expressions 2007).

The photocathode is held at a high negative voltage (-1000V to -2000V) which decreases to 0V at the last dynode (a voltage difference exists between each dynode). This change in voltage is used to accelerate electrons from the photocathode to the anode as well as for amplification purposes. When a photon hits the photocathode (a film of metal), one single electron is ejected and accelerated towards the first dynode (due to the voltage difference). Once the electrons hit the first dynode 5 to 20 times the number of electrons are ejected and accelerated toward the second dynode due to the voltage difference. The amplification is repeated until the last dynode is reached and the signal can be read at the output. The amplification is dependent on the voltage differences between the photocathode and the dynodes. A higher voltage difference stands for higher acceleration which leads to the ejection of more electrons and to increased amplification and thus higher sensitivity.

There are three timing characteristics that are used to describe PMTs: transit time, rise time, and transit time spread. Transit time is the period between the time when a photon hits the photocathode and the detection of the magnified signal at the anode. Rise time is the time that takes for the current at the anode to rise from 10 to 90% of the final value. Although important, both transit and rise times are not the main consideration when choosing a PMT for a frequency domain device. Transit time spread is the most significant feature for time resolved spectroscopy.

It is important to recognize that not all the electrons arrive at the anode simultaneously, the time between the arrival of the first electron and the last

electron is called the transit time spread. The transit time spread is a major source of error for time resolved measurements. There are two causes for transit time spread: the PMT geometry and the color effects (Lakowicz 2006). Electrons follow a path within the PMT which depends on the photocathode and dynodes geometries. Since the electrons are ejected from different locations on the photocathode and dynode, they will follow a slightly different path to the anode. As a result, all electrons will not arrive at the same time. Better PMT geometries can reduce the transit time spread but not eliminate it.

The color effects contribution to transit time spread is due to the wavelength dependency of the photocathode (Rayner and others 1976; Wahl and others 1974). The wavelength of the incident photon causes an electron of certain energy to be ejected from the photocathode. The energy of the electron is dependent on the wavelength of the incident photon. Since electrons of different energies follow different trajectories to the anode, this phenomenon increases the transit time spread. A correction to the color effects is possible through the use of fluorescence reference lifetime(Lakowicz and others 1981; Mauzerall and others 1985; Thompson and Gratton 1988).

Multi-channel plate detector (MCP)

MCP consists millions of micro meters diameter tubes parallel to each other. Each one of these tubes acts as a detector (electron channel) and as a consequence of its unique geometry the transit spread time is significantly

reduced. Nevertheless, reference lifetime standards are still needed even when using MCPs (vandeVen and others 2005).

PMT's and MCP's have a frequency response that limits the signals that can be detected. Most PMT's can reliably detect signals below 200MHz while MCP's can perform well into the GHz frequencies (Lakowicz and others 1988). The PMT R-928 which was used in this research is best suited to work a frequencies under 200MHz but can still be used to measure signals up to 400MHz (Lakowicz 2006).

4.5 Fluorescence reference lifetime standards

Fluorescence reference lifetimes standards are used in the frequency domain method to correct for the PMT transit time spread color effects, and for the time delay in cables and electronic circuits. The reference lifetime is measured under the same conditions (same excitation source and emission filters) as the sample and the data is used for correction. The phase shift (Φ_R) and modulation (m_R) of the reference lifetime are used in Equations 32 and 33 to correct for the color effects (Lakowicz 2006).

$$\phi_\omega = \phi_\omega^{obs} + \phi_R \tag{32}$$

$$m_\omega = m_\omega^{obs} \times m_R \tag{33}$$

Where Φ_ω and m_ω are the corrected phase and modulation values and Φ_{obs} and m_{obs} are the sample's observed phase and modulation values. The observed phase shift is measured relative to the reference lifetime and so the observed phase shift is smaller than the corrected phase shift. Similarly, the observed modulation value which is the ratio of the corrected value and the reference lifetime modulation.

There are several characteristics that a fluorophore must exhibit in order to be used as a reference lifetime standard. The fluorophore must have a known single exponential lifetime that is independent of excitation and emission wavelengths (Boens and others 2007). The fluorescence lifetime must be short (around 1ns) in order to avoid oxygen quenching (Barrow and Lentz 1983). A large stokes shift helps reducing excitation and emission bands overlap. Since the sample and reference are measured under the same conditions the selected reference must exhibit the same excitation and emission wavelengths as the sample. It is also highly recommended that the standard is commercially available and that further purification is not required.

In order to promote the use of frequency domain devices a big selection of reference lifetime standards that cover both the visible spectrum as well as the picoseconds and nanoseconds timescales must be available. However, not many reference lifetime standards are available when one is interested in the picosecond timescale (Boens and others 2007). Recently, an attempt to establish a set of commercially available standards by measuring and comparing the results of the standards in nine different laboratories was made (Boens and

others 2007). The researchers established twenty standard lifetime references however, only 3 of these standards exhibit a picosecond lifetimes. An earlier effort to establish a set of picoseconds reference lifetime dyes was done by Lakowicz and others (1991). Lakowicz and others (1991) worked with a group of diethyl-amino-stilbene derivatives which exhibited single exponential lifetimes ranging from 880 to 57 picoseconds and covering wavelengths from 260 to 430nm (Lakowicz and others 1991). Unfortunately these substances are still not commercially available and must be synthesized and purified. Other known picoseconds reference lifetimes that are available are listed in Table 1.

Fluorophore	Solvent	Excitation (nm)	Emission (nm)	Lifetime (nsec)	Reference
Rose Bengal	Water	548	567	0.091	(ISS 2007)
cy3	Pbs	548	562	0.3	(ISS 2007)
Cy3.5	Pbs	581	596	0.5	(ISS 2007)
Indocyanine-green	Water	780	820	0.52	(ISS 2007)
Erythrosine B	Water	488-568	550-580	0.089	(Boens and others 2007)
Erythrosine B	Methanol	488-568	550-590	0.47	(Boens and others 2007)
p terphenyl	Cyclohexane	290-315	330-390	0.98	(Boens and others 2007)

Table 1: Fluorophores exhibiting single exponential picosecond fluorescence lifetimes. Pbs=Phosphate buffered saline

To the best of our knowledge, no commercially available picoseconds reference lifetime standard exists which can be excited at the wavelengths between 400 to 460nm. A commercially available reference lifetime standard at these wavelengths will help cover an important gap in the visible spectrum for the investigation of picosecond timescale processes.

CHAPTER 5

Molecular Rotors

One fluorescent mechanism that doesn't rely on π to π* transfer is intramolecular charge transfer (ICT). In ICT fluorophores, one part of the molecule act as electron donor, the other part as an electron acceptor in the excited state. A well explored sample is 1-dimethyl amino benzo nitrile (DMABN). Lippert and others (1962) found that DMABN unexpectedly possessed two fluorescence bands: an anticipated band at 350nm (normal for a benzene derivative) and an irregular band at a much longer wavelength. The red shifted irregular fluorescence band showed an increase in intensity with increased polarity of the solvent. Lippert and others (1962) attributed this behavior to two electronic states: L_A and L_B. He proposed that in nonpolar solvent the L_B state (corresponding to the 350nm band) was at lower energy than the L_A state (corresponding to the red shifted band) and so photon emission occurs from the L_B 350nm emission band. In polar solvents, the L_A state is stabilized (lower energy level) and gets populated. Thus, photon emission is observed at the red shifted band.

Eleven years later Grabowski and others (1973) offered a different explanation for the dual band emission. He believed that a twisted intramolecular charge transfer (TICT) mechanism is responsible for the dual band appearance (Grabowski and others 1973). The L_B state arises from the planar structure of DMABN and the transition to the L_A state is due to twisting of the dimethylamino group as shown in Figure 15 (Grabowski and others 1973).

The twisted state is of lower energy than the planar state and is energetically favorable (Figure 15). Hence, the probability of TICT formation is higher. De-excitation from the twisted state results in the red shifted fluorescence band. However, a polarity dependent energy barrier between the planar and the twisted conformations exists (Figure 15). In non-polar solvents the energy barrier significantly increases, causing a higher probability of de-excitation from the planar state (resulting in the 350nm fluorescence band). As polarity increases, the energy barrier is reduced and emission from the higher fluorescence band is observed. Increased polarity induces a stronger red shifting of the TICT state emission bandwidth.

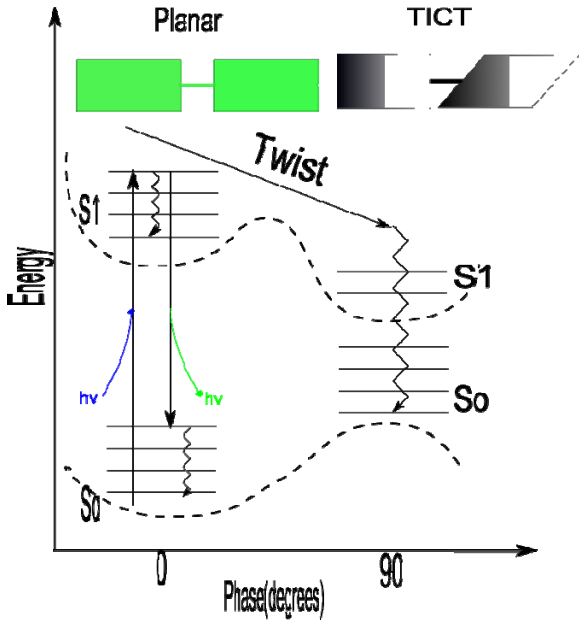

Figure 15: Energy diagram of TICT molecule.

A sub group of TICT forming molecules commonly referred to as molecular rotors exhibits only a single emission band. A member of this sub-group, 9-(2-carboxy-2-cyanovinyl) julolidine (CCVJ), is composed of a julodine

group that acts as the donor and a nitrile group that acts as the electron acceptor. In CCVJ the twisting occurs around the C=C double bond (Figure 16).

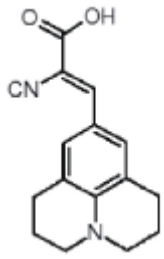

Figure 15: Chemical structure of CCVJ. The julodine nitrogen acts as the donor and the nitrile group acts as the electron acceptor.

Forster and Hoffmann (1971) studied the intensity dependency of dyes that exhibit intramolecular rotation (crystal violet is one of these dyes) on the environment's free volume. These dyes have comparable photo-physical to CCVJ. They found that following photon absorption there are two possible de-excitation pathways:

1) De-excitation from the planar state resulting in photon emission.
2) Twisting of the molecule followed by non-radiative de-excitation from the twisted state.

The energy barrier between the planar and twisted conformations is dependent on the free volume of the environment. Thus, the emission intensity and the quantum yield are inversely proportional to CCVJ's free volume surrounding (Forster and Hoffmann 1971). As established in Chapter 1 (Equation 4) there is a direct relationship between free volume and viscosity therefore CCVJ's emission intensity and quantum yield exhibit a power law relationship with regard to the environment's viscosity. Forster and Hoffmann (1971) derived a power law

relationship commonly known as the Forster-Hoffmann Equation that describes the relationship between the quantum yield and the environment's viscosity.

$$\log\phi = x \cdot \log(\eta) + C \tag{34}$$

Where x is a dye constant which theoretically equals 0.6 in the case of CCVJ and C is a temperature dependent constant.

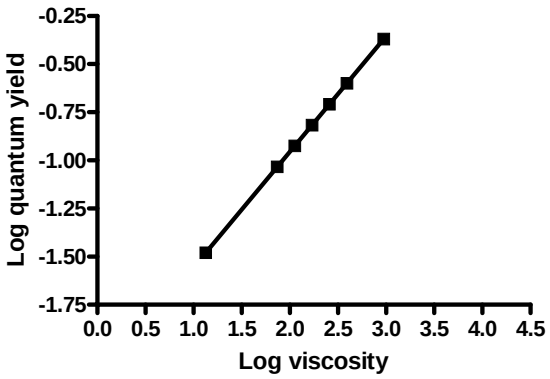

Figure 17: Log-log plot of CCVJ's quantum yield Vs. viscosity.

An alternate form of the Forster-Hoffman Equation is:

$$\phi = C \cdot \eta^{x} \tag{35}$$

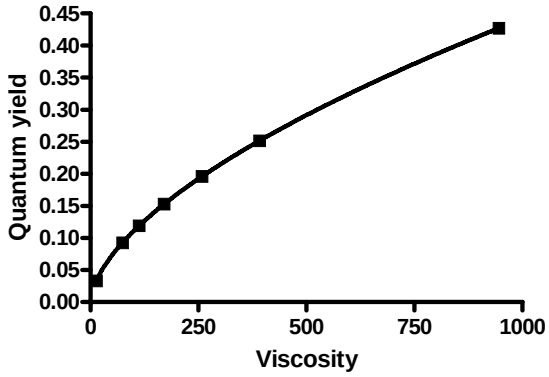

Figure 18: Power law fit of CCVJ's quantum yield Vs. viscosity.

The fluorescence quantum yield is proportional to the fluorescence. However, the measured intensity is also dependent on dye concentration, instrument errors, and other factors. With some adjustments of Equation 35, the quantum yield can be substituted by fluorescence intensity and so the viscosity can be directly calculated from the intensity (Haidekker and others 2002).

$$\eta = \left(k \cdot I\right)^{\frac{1}{X}} \tag{36}$$

Where I stands for the measured intensity and k is a constant that accounts for instrument properties and temperature.

Molecular rotors were employed as environmental probes to study: tubulin structure (Kung and Reed 1989), phospholipids bilayers microviscosities (Kung and Reed 1986), microviscosities of polymer metrics (Loutfy 1986), attachment to antibodies (Iwaki and others 1993), and blood plasma viscosities (Akers and others 2005; Haidekker and others 2002). Most recently, CCVJ was

used to determine the viscosity changes of blood plasma (Akers and others 2005; Haidekker and others 2002). The novel viscosity probe showed great promise however, some difficulties must be overcome before the probe can be used in clinical settings. Haidekker (2002) used steady state spectroscopy and used Equation 32 to determine the viscosity. He found that errors occurring as a result of concentration inaccuracies and fluid optical properties must be accounted for or eliminated. Time resolved spectroscopy offers an immediate solution to this problem since the fluorescence lifetime is typically not affected by the probe's concentration (Lakowicz 2006).

Some time resolved studies involving CCVJ were done by Iwaki and others (1993). CCVJ was used as an indicator to show if it was attached to antibodies (Iwaki and others 1993). The probe's quantum yield and fluorescence lifetime showed a dramatic change upon binding to the antibody. The fluorescence lifetime followed a single exponential decay where free and bound fluorescence lifetimes were found to be 62 and 388 picoseconds respectively (Iwaki and others 1993). This earlier study by Iwaki and others(1993) demonstrates that CCVJ exhibits a single exponential decay in the picoseconds timescale, independent on whether deexcitation occurs from the planar or the TICT states.

A model describing CCVJ's fluorescence lifetime as a function of viscosity can become a useful tool in tracing blood plasma anomalies and investigation of micro environments. This study tries to model the fluorescence lifetime viscosity relationship as well as testing if CCVJ can be applied as a "tunable" picoseconds reference lifetime standard

CHAPTER 6

Challenges in the Fluorescent Lifetime Measurements Approaches of CCVJ in Different Viscosities

Frequency domain measurements employs reference lifetime standards to correct for the color effects. In some cases, especially when trying to measure processes on a picoseconds timescale it is very hard to find a suitable reference. This research initially employed scatterers in different concentrations as references to simulate zero fluorescence lifetimes. The scatterers that were used included: $Si0_2$ in water, Intra lipid in water, Dextrin in water, bovine albumin in Pbs. This approach resulted in distorted signals which yielded very high X^2 values (Figure 19). Scatterers correct only for the delay time introduced by cables and electronic circuits but fail to correct for the spectral response of PMTs (Lakowicz 2006). The results validated the need for a fluorescent reference lifetime standard with the same excitation and emission wavelengths and a known fluorescence lifetime to correct for the PMT's spectral response (color effects).

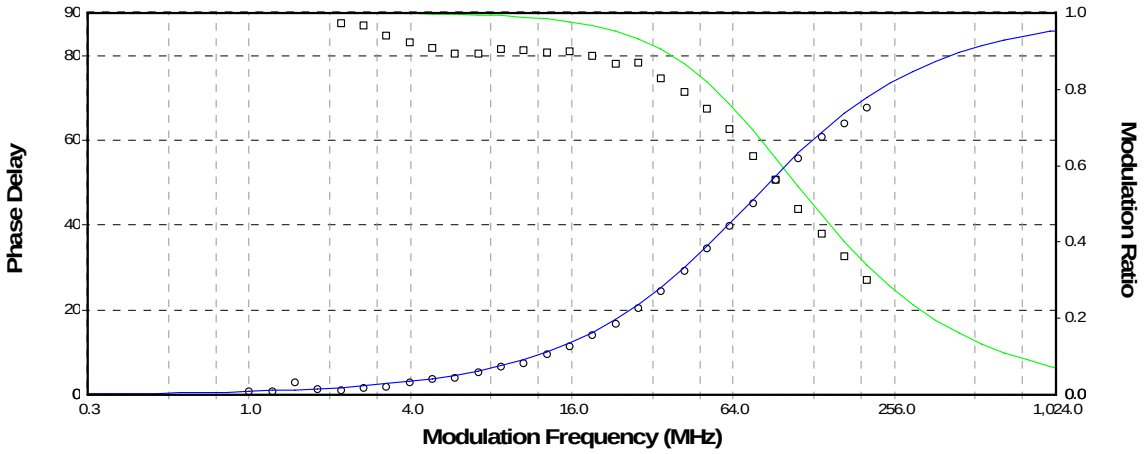

Figure 19: SiO2 in water was used to measure Coumarin 6 in ethanol (known lifetime 2.5nsec). 10-200MHz τ=2.18nsec X^2=107.73

A second experiment involved using Coumarin 6 in ethanol (τ=2.5nsec), which has similar excitation and emission bands as CCVJ, as a reference lifetime standard. The main obstacle in this approach is the relatively long fluorescence lifetime of the standard which is not suitable for the measurement of picoseconds processes (exhibits a different frequency response). The results in this case would stipulate that CCVJ in glycerol exhibited a double exponential decay, τ_1 and τ_2, which were assumed to be viscosity and polarity dependent. These results contradicted Iwaki and others (1993) who found that CCVJ exhibits a single exponential decay using a streak camera device (Iwaki and others 1993). Trying to use Coumarin 6 to measure CCVJ in lower viscosities (i.e. very short CCVJ lifetimes) resulted in distorted measurement so CCVJ in glycerol was used as a reference lifetime instead. The mean fluorescent lifetime of CCVJ in glycerol (0.9nsec) was used to represent the fluorescence lifetime. The measurements of CCVJ in lower viscosities (using CCVJ in glycerol as a reference) continued to

show a double exponential decay. But, the decay times, τ_1 and τ_2, showed no consistent trend. Nevertheless, the mean lifetime (a weighted sum of τ_1 and τ_2) could be used to model a power law relationship between viscosity and the mean fluorescence lifetime. This approach was abandoned because:

1) The mean lifetime showed inconsistencies at the lower viscosities (below 5mPa*s).

2) Inconsistent trends of the τ1 and τ2.

3) Reference lifetime standards must exhibit single exponential decay.

4) Mean lifetimes are rarely used to model processes.

An important lesson from this experiment was to use CCVJ as reference lifetime standard (once it was found to have a single exponential decay).

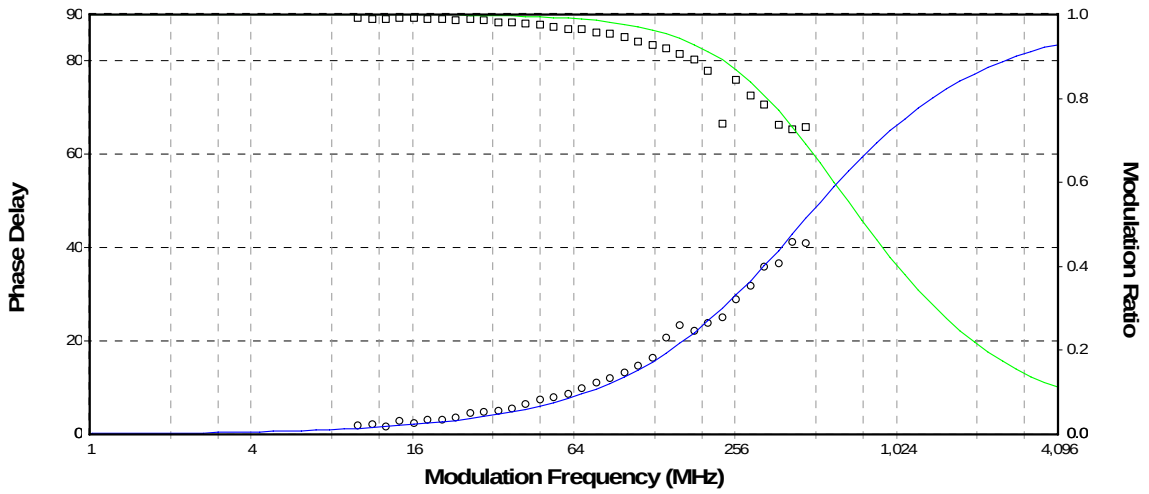

Figure 20: Coumarin 6 in ethanol used to measure CCVJ in 70% glycerol 30% ethylene glycol 10-470MHz τ=0.353nsec X^2=60.95.

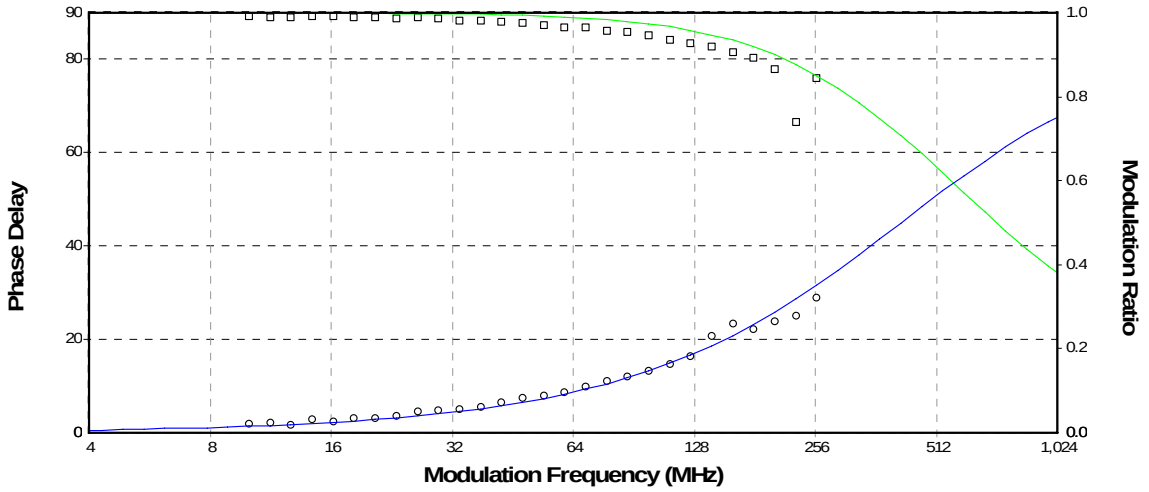

Figure 21: Coumarin 6 in ethanol used to measure CCVJ in 70% glycerol 30% ethylene glycol 10-260MHz τ=0.38nsec X^2=41.24.

In the search for a suitable reference lifetime standard, two picoseconds lifetime standards were purchased. Rose Bengal in water has a fluorescence lifetime of 0.091 nsec and Erthrosine B a fluorescence lifetime of 0.089nsec. Both dyes failed as a lifetime reference standard to measure CCVJ in different viscosities since they couldn't be excited by 405 or 440nm light (they could be excited at around 500nm). Finally, the lifetime reference 1,4-Bis(4-methyl-5-phenyl-2-oxazolyl)benzene (DPOPOP) with fluorescence lifetime of 1.45nsec (in methanol) could be used to measure CCVJ in different viscosities. DPOPOP could only be used with the 405nm laser diode due to its absorption spectra. Several measurements of CCVJ using DPOPOP as a reference are given below.

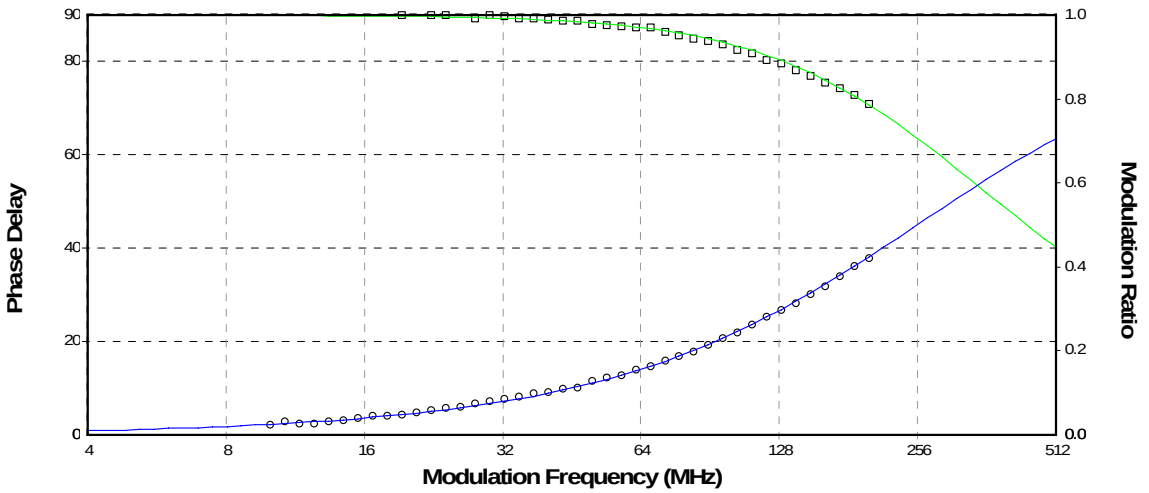

Figure 22: DPOPOP in methanol used as a reference to measure CCVJ in 100% glycerol 10-200MHz τ=0.624nsec X^2=1.65.

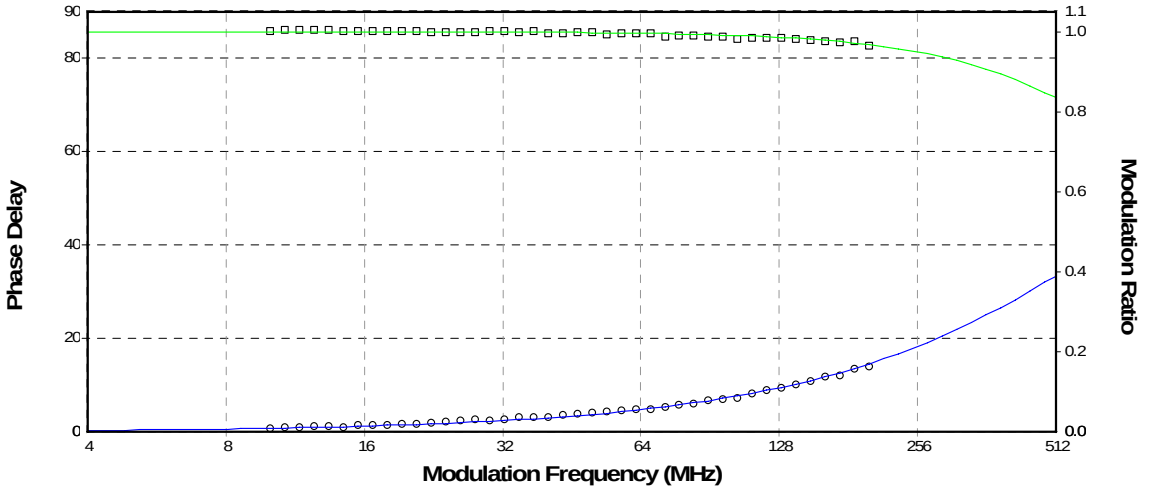

Figure23: DPOPOP in methanol used as a reference to measure CCVJ in 50% glycerol 50% ethylene glycol.10-200MHz τ=0.206nsec X^2=1.3.

A dramatic improvement in the measurements quality of CCVJ was observed when DPOPOP was used as a lifetime reference. The improvement is due to DPOPOP short fluorescence lifetime as well as to the fact that it could be excited at 405nm and observed at the same emission wavelength as CCVJ (through a 440

long-pass filter). Due to its superior qualities, DPOPOP was used as a primary reference lifetime in this research.

CHAPTER 7

Key Experiments

7.1 Materials and methods

Ethanol spectrophotometric grade, ethylene glycol, spectrophotometric grade ≥ 99%, glycerol, spectrophotometric grade ≥ 99.5%, methanol, ACS spectrophotometric grade ≥ 99.9%, dimethyl sulfoxide, ACS spectrophotometric grade ≥ 99.9%, and water for UV-spectroscopy, were purchased from Sigma–Aldrich and used as solvents.

Dyes that were used included: CCVJ (purchased from Sigma–Aldrich), Lucifer yellow (LY), 1,4-Bis(4-methyl-5-phenyl-2-oxazolyl)benzene (DPOPOP), Coumarin 153 (C153), and Coumarin 6 (C6). To create stock solutions CCVJ was dissolved in dimethyl sulfoxide, LY was dissolved in water, C153 was dissolved in methanol, DPOPOP was dissolved in toluene, and C6 was dissolved in ethanol. Steady state measurements were performed using a Fluoromax 3 spectrofluorometer (Jobin Yvon) and time resolved measurements were performed using Chronos 2 time-resolved spectrometer (ISS). For the X^2 determination the uncertainties $\delta\Phi$ and δm were given the values of 0.2^o and 0.005, respectively as recommended by Lakowicz (2006). All steady state and time resolved measurements were done in glass cuvettes and at room temperature and the fluorescence lifetimes were determined using the X^2 test.

The research objectives were to characterize the molecular rotor CCVJ for its fluorescence lifetime viscosity dependency and evaluate its possible use as a reference lifetime standard.

7.2 Absorption and emission spectra

CCVJ was dissolved in DMSO to create a stock solution with a 10 mM concentration. Ten micro liters of the stock were added to 10 ml of glycerol which were mixed for an hour at room temperature. Absorption spectra was obtained by observing the emission at 490nm and varying the excitation light from 360 to 480nm. Emission spectra of 10 micro molar CCVJ in glycerol were obtained by using Fluoromax–3 with 440nm excitation light.

Results

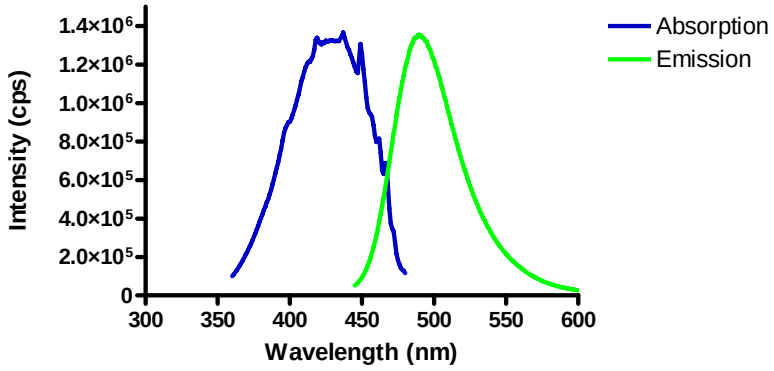

Figure 24: Absorption and emission spectra of CCVJ in glycerol.

CCVJ in glycerol exhibits a Stoke's shift of 53nm where ideal absorption occurs at 437nm and peak emission is at 490nm.

7.3 Fluorescence lifetime as a function of probe's concentration

Three samples of 5, 7, and 10 micro molar CCVJ in glycerol were made and mixed for an hour at room temperature. Steady state measurement with 405nm excitation light was performed for each sample and the averaged fluorescence intensity peak value for each concentration was calculated. For each of the samples, time resolved measurements with excitation source of 405nm and 440nm long pass emission filter were done as well. The results were analyzed using the X^2 test and the obtained fluorescence lifetimes for each concentration were averaged. In the time resolved measurements, DPOPOP in ethanol was used as a reference lifetime and the frequency of the modulated light was varied between 10 and 250MHz.

Results

CCVJ's fluorescence lifetime and intensity as a function of dye concentration

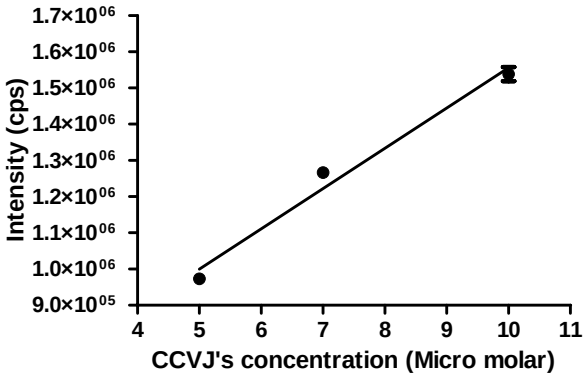

Figure 25: Intensity of 5, 7, and 10 Micro molar CCVJ in glycerol.

Linear regression was used to show that increasing CCVJ's concentration results in increased intensity (Figure 25). The slope of the line was found to be 111400 ± 663 with R^2-0.975.

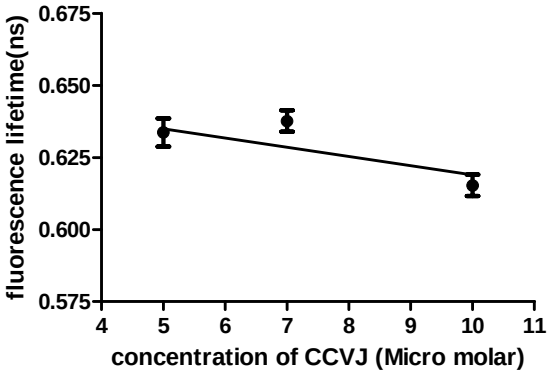

Figure 26: Fluorescence lifetime of 5, 7, and 10 Micro molar CCVJ in glycerol.

Linear regression was used again to describe CCVJ's fluorescence lifetime and concentration relationship (Figure 26). The slope of the line was found to be -0.003965 ± 0.001453 with R^2=0.5155.

The intensity showed an increase of 56% due to increased concentration while fluorescence lifetime varied by only 3%. The small decrease in the fluorescence lifetime with increased concentration is attributed to inner filter effects and so it is recommended to work with concentrations below 10 Micro Moles. These results validate that by using fluorescence lifetime measurements we can eliminate concentration inaccuracies.

7.4 Fluorescence lifetime as a function of viscosity

A viscosity gradient (13.35mPa*s to 945mPa *s) was achieved by using mixtures of glycerol and ethylene glycol. For each viscosity, three samples of 7 micro molar CCVJ were made. In order to reduce concentration inaccuracies, CCVJ was first added to ethylene glycol and mixed for an hour at room temperature. The pre-stained ethylene glycol was then added to glycerol and ethylene glycol as described in Table 2 and the resulting mixture was mixed for one more hour. Steady state measurement with 405nm excitation light were performed and the averaged fluorescence intensity peak value for each viscosity was calculated. For each of the samples, time resolved measurements with excitation source of 405nm and 440nm long pass emission filter were done as well. X^2 tests were performed and the obtained fluorescence lifetimes for each viscosity were averaged. A correlation between the obtained fluorescence lifetimes and corresponding intensities was done.

DPOPOP in ethanol and CCVJ in 100% glycerol, 60% glycerol 40% ethylene glycol, 40% glycerol 60% ethylene glycol, were used as a reference lifetimes in the time resolved measurements. When DPOPOP was used as reference lifetime, the frequencies of the modulated light varied between 10 and 250MHz, but for the CCVJ reference lifetimes, the frequencies varied between 10 and 450MHz.

Glycerol/ Ethylene Glycol percentage	Glycerol (ml)	Ethylene glycol (ml)	Pre-stained Ethylene Glycol (70 Micro molar) (ml)	Total Volume (ml)	Final Concentration (Micro Molar)
80	16	2	2	20	7
70	14	4	2	20	7
60	12	6	2	20	7
50	10	8	2	20	7
40	8	10	2	20	7
0	0	18	2	20	7

Table 2: Preparation method of CCVJ in different viscosities.

The data obtained using CCVJ as reference lifetime standard was also analyzed by the X^2 test using only 3 data points at 10, 40, and 120 MHz to reduce the measurement time.

Results

CCVJ's intensity and fluorescence lifetime as a function of viscosity

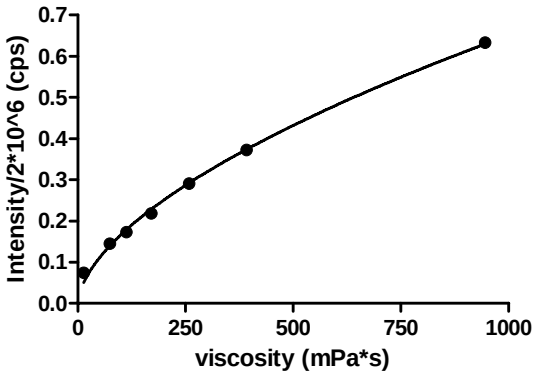

Figure 27: Power law fit of CCVJ's intensity in different viscosities using a 405nm excitation wavelength.

A power law fit was used to describe CCVJ's intensity and viscosity relationship (Figure 27). The nonlinear regression resulted in Y=0.01093*X^O.5917 with R^2=0.9949.

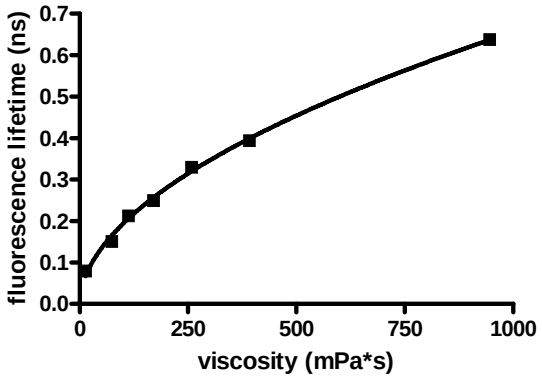

Figure 28: power law fit of CCVJ's fluorescence lifetimes in different viscosities. DPOPOP was used as a reference lifetime and both sample and reference were excited by 405nm laser diode.

DPOPOP was used as a reference lifetime standard and CCVJ's frequency response to modulated light between 10 and 200MHz was analyzed to obtain the results given in Figure 28 (X^2 values are given in Table). A power law fit was used to describe CCVJ's fluorescence lifetime and viscosity relationship. The nonlinear regression resulted in Y=0.01684*X^0.5302 where R^2=0.9956. When CCVJ in 100% glycerol and 60% glycerol were used as reference lifetimes, modulated light at frequencies between 10 to 300MHz was used to excite the sample. Due to the different lifetime standard a slightly different result was obtained (Figure 29).

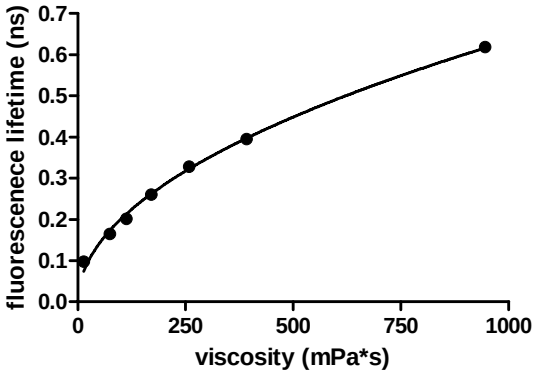

Figure 29: Power law fit of CCVJ's fluorescence lifetimes in different viscosities. CCVJ was used as a reference lifetime and both sample and reference were excited by 405nm laser diode.

Again a power law fit was used to describe CCVJ's fluorescence lifetime and viscosity relationship (Figure 29). The nonlinear regression resulted in $Y=0.02022*X^{0.4988}$ where $R^2=0.9932$. Although the R^2 values are above 0.99 for both fluorescence lifetimes measured by using DPOPOP and CCVJ as reference standards, the latter results were found more accurate for the following reasons.

1) CCVJ measurements contained 50% more information (300MHz instead of 200MHz).
2) CCVJ acts as better lifetime standard since it has a shorter lifetime than DPOPOP and its emission band in different viscosities is almost the same as the measured sample (better correction for the color effects).

The averaged fluorescence lifetimes obtained for the different viscosities are given in Table 3.

Viscosity (mPa*s)	Averaged fluorescence lifetime (ns) 10-200MHz (DPOPOP as reference)	Averaged fluorescence lifetime (ns) 10-300MHz (CCVJ as reference)
945	0.638	0.618
391.4	0.394	0.395
258.11	0.330	0.328
170.21	0.249	0.261
112.25	0.213	0.201
74.02	0.151	0.165
13.35	0.080	0.098

Table 3: Averaged fluorescent lifetimes of CCVJ in different viscosities obtained by using DPOPOP and CCVJ as reference lifetime standards.

We correlated the fluorescence lifetime and emission intensity and determined a significant linear fit R^2=0.9927 (Figure 30).

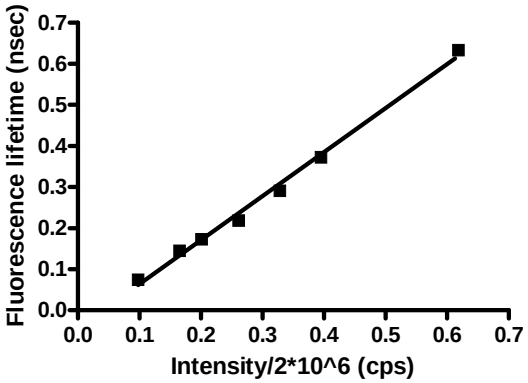

Figure 30: Correlation between fluorescence lifetime and intensity data of 7 Micro Molar CCVJ in different viscosities.

The high R^2 confirms that CCVJ's fluorescence lifetime can be used as a viscosity measurement tool.

7.5 Fluorescence lifetime analysis using only 3 fixed modulation frequencies

X^2 analysis of the phase modulation data obtained while using CCVJ as a reference lifetime was done for data points between 10 and 200MHz(42 data points). The measurement time required to obtain this data was between 5 and 7 minutes. The same analysis was done using only three frequencies (10, 40, 120 MHz). The required measurement time to obtain this data was reduced to 30 seconds. The averaged fluorescence lifetimes and X^2 values are given in Table 4.

Viscosity (mPa*s)	Averaged fluorescence lifetime (ns) 40, 80, and 120 MHz (CCVJ as reference)		Averaged fluorescence lifetime (ns) 10-200MHz (CCVJ as reference)	
945	0.612	X^2=1.283	0.618	X^2=0.957
391.4	0.394	X^2=1.402	0.379	X^2=1.303
258.11	0.325	X^2=1.327	0.324	X^2=1.233
170.21	0.267	X^2=1.187	0.265	X^2=1.063
112.25	0.204	X^2=0.833	0.203	X^2=0.723
74.02	0.167	X^2=0.747	0.168	X^2=0.877
13.35	0.096	X^2=0.393	0.097	X^2=0.733

Table 4: CCVJ's fluorescent lifetimes and X^2 values in different viscosities obtained by using 3 fixed frequencies compared to results obtained with 10-200MHz frequency modulation range.

The 3 points measurements show only a slight variation in fluorescence lifetimes with a good X^2 values (below one in many cases). These results confirm that short

time (30 seconds) viscosity measurements using CCVJ's fluorescence lifetimes are possible.

Since CCVJ was successfully used as a picoseconds reference lifetime standard in the previous experiments, several more experiments were designed and conducted to help establish it as a tunable picoseconds reference lifetime standard.

7.6 Establishing of CCVJ as a reference lifetime standard

The X^2 values obtained for measurements of CCVJ in different viscosities using DPOPOP and CCVJ as a reference lifetime were compared to show the superiority of CCVJ as a reference. Frequency responses using DPOPOP and CCVJ as standards are shown for the same reasons. Characterization of CCVJ as reference lifetime standard is followed. A reference lifetime standard must exhibit fluorescence lifetime independent of excitation wavelength. In order to check CCVJ's fluorescence lifetime for its wavelength dependency time resolved measurements were done using a 440nm laser diode. For each viscosity three samples of 7 micro molar CCVJ solutions were made between 13.35mPa*s and 945mPa *s (same samples as in the 405 excitation, Table 2). For each of the samples, time resolved measurements with excitation source of 440nm and 455nm long pass emission filter were done as well. X^2 tests were performed and the obtained fluorescence lifetimes for each viscosity were averaged. CCVJ was applied as a reference lifetime standard and was used to measure four single exponential fluorophores with known fluorescence lifetime. The selected fluorophores had excitation and emission wavelengths similar to CCVJ (Table 5).

Three samples of each fluorophore were made in the corresponding solvent (Table 5). For each sample, time resolved measurements with an excitation source of 405nm and 440nm long pass emission filter were done as well as measurements with an excitation source of 440nm and 455 nm long pass emission filter. X^2 tests were performed and the obtained fluorescence lifetimes for each concentration were averaged and compared to the known value. CCVJ in 100% glycerol, 60 % glycerol 40 % ethylene glycol , 40 % glycerol 60% ethylene glycol, and ethylene glycol were used as reference lifetimes.

Fluorophore	Solvent	Known fluorescence lifetime (nsec)	Modulation frequency (MHz)	Reference	EX (nm)	EM (nm)
Dpopop	Ethanol	1.45	10-200	ISS	300-400	390-560
Coumarin 6	Ethanol	2.5	10-120	ISS	460	505
Coumarin 153	Water	4.18	1-80	(Boens and others 2007)	295-442	495-550
Lucifer yellow	Water	5.1	1-60	(Mishra and others 2004)	428	535

Table 5: Fluorophores that were used to validate CCVJ's ability to perform as a reference lifetime standard. C153 fluorescence lifetime is based on frequency domain measurements.

Results

Comparison of DPOPOP and CCVJ'S performance as reference lifetimes

The performance of CCVJ as reference lifetime standard was evaluated by comparing the X^2 values of CCVJ and DPOPOP (Table 6).

Viscosity (mPa*s)	Averaged X^2 values (DPOPOP as reference) 10-200MHz	Averaged X^2 values (CCVJ as reference) 10-200MHz	Averaged X^2 values (CCVJ as reference) 10-300MHz
945	0.817	0.957	1.957
391.4	1.207	1.303	1.653
258.11	1.847	1.233	1.587
170.21	1.607	1.063	2.177
112.25	1.247	0.723	0.897
74.02	2.103	0.877	1.087
13.35	1.947	0.733	0.933

Table 6: Averaged X^2 values of CCVJ in different viscosities obtained by using DPOPOPO and CCVJ as reference lifetime standards.

When increasing the frequency above 200MHz DPOPOP functioned poorly as a reference lifetime. However, when CCVJ was used as a reference lifetime, frequencies of 300MHz were achieved for all viscosities with X^2 values below 2 in most cases (Table 6). Clearly, more high- frequency information can be gained by using CCVJ as reference lifetime standard.

When comparing CCVJ and DPOPOP X^2 values for the same range of frequencies (10-200MHz) CCVJ exhibited a lower X^2 in almost all cases (Table 6).

The biggest advantage of using CCVJ as a reference lifetime standard is that more high-frequency information was obtained. The signal's noise level was reduced due to CCVJ's superiority in correction for the color effects and lower modulation at higher frequencies. In some cases, results at 400MHz and even 450MHz were obtained, doubling the amount of information (Figure 31).

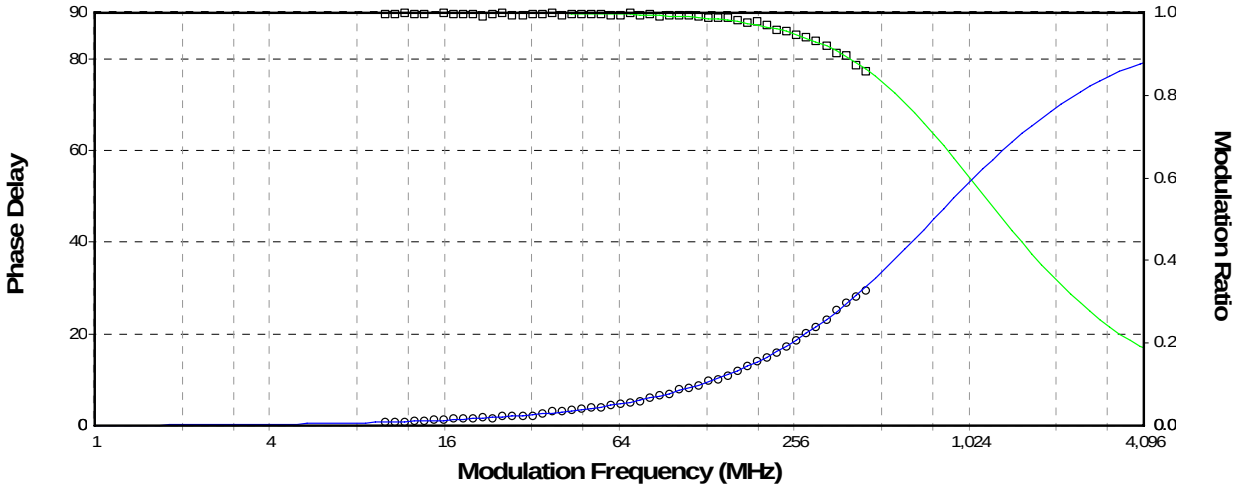

Figure 31: Frequency response of CCVJ in 50% glycerol 50% ethylene glycol.
X^2=0.86 τ=0.206nsec 10-450MHz
Reference lifetime =CCVJ in 60% glycerol 40% ethylene glycol (o.395nsec)

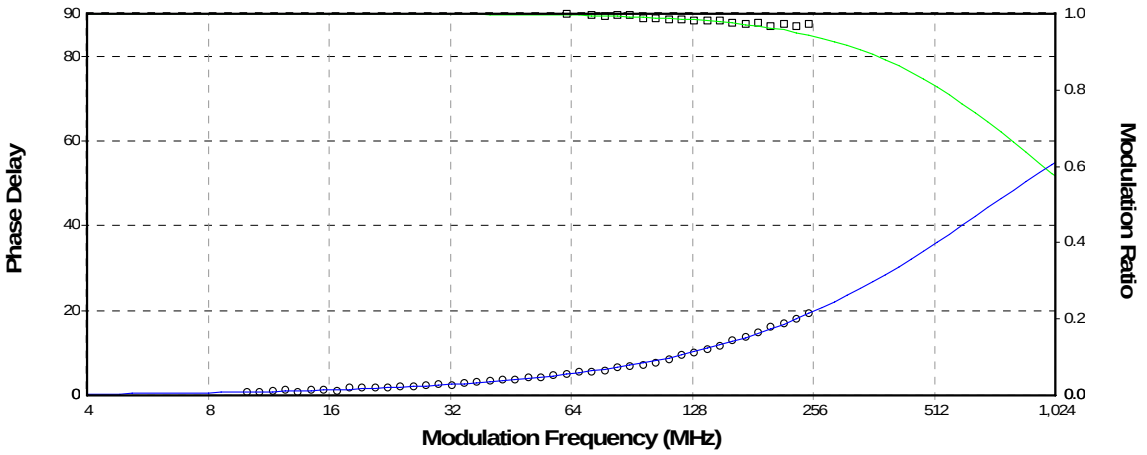

Figure 32: Frequency response of CCVJ in 50% glycerol 50% ethylene glycol. X^2=2.1 τ=0.222nsec 10-250MHz Reference lifetime =DPOPOP (1.45nsec)

Establishing CCVJ as a reference lifetime standard

CCVJ fluorescence lifetimes were measured using 405nm and 440 nm laser diodes. The fluorescent lifetimes for both wavelengths are given in Table 7.

Viscosity (mPa*s)	405nm excitation averaged fluorescence lifetime (ns)10-300MHz (CCVJ as reference)	440nm excitation averaged fluorescence lifetime (ns) 10-300MHz (CCVJ as reference)
945	0.618	0.630
391.4	0.395	0.411
258.11	0.328	0.315
170.21	0.261	0.245
112.25	0.201	0.202
74.02	0.165	0.159
13.35	0.098	0.089

Table 7: Averaged florescent lifetimes of CCVJ in different viscosities obtained by using 405 and 440nm excitation sources.

The fluorescence lifetimes show only a slight variation between 405 and 440nm excitation wavelengths. These variations may be due to mixtures and device errors. For all practical applications (due to the fact that only small variations were observed), we can conclude that CCVJ fluorescence lifetime is independent of excitation wavelength.

7.7 Measurement of fluorophores with known fluorescence lifetime using CCVJ in 5 different viscosities as reference lifetime standard

Four different fluorophores with a single exponential decay and known lifetime were measured using CCVJ in different viscosities as reference lifetime standard (DPOPOP couldn't be excited using 440nm light source and was measured only at 405nm). The lifetime measurements were done using 405nm and 440nm laser diodes to check if CCVJ can be used as reference lifetimes at both wavelengths. The results are shown in Figures 33 and 34.

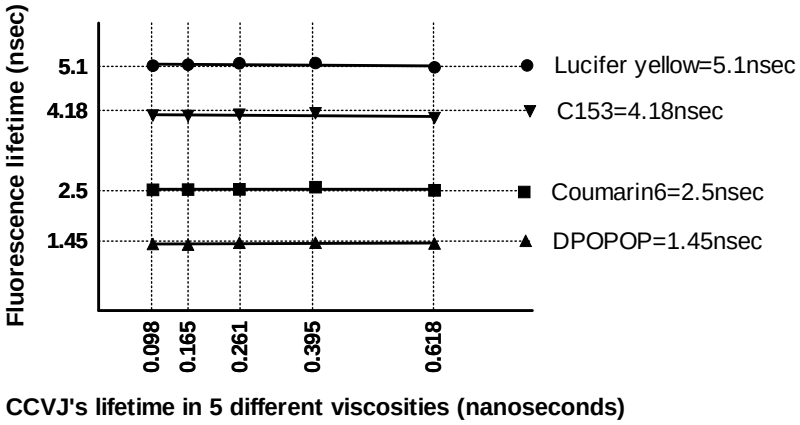

Figure 33: CCVJ in 5 different viscosities used as a reference lifetime standard to measure fluorescent dyes with known fluorescent lifetimes. Both sample and reference were excited by 405nm laser diode.

The linear lines in Figure 33 showed no significant deviation from zero which means that the measured fluorescence lifetimes are independent from the reference lifetimes used.

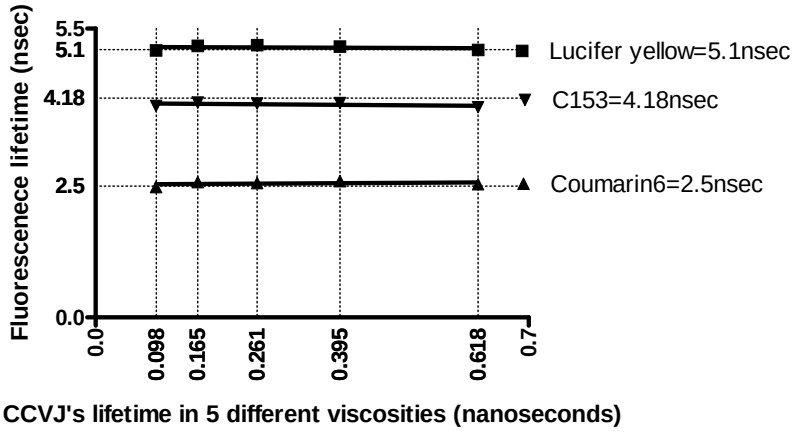

Figure 34: CCVJ in 5 different viscosities used as a reference lifetime standard to measure fluorescent dyes with known fluorescent lifetimes. Both sample and reference were excited by 440nm laser diode.

The linear lines in Figure 34 showed no significant deviation from zero which means that the measured fluorescence lifetimes are independent from the reference lifetimes used.

The averaged X^2 values for each of the measurements are given in Tables 8 and 9.

CCVJ fluorescence lifetime in 5 different viscosities (nsec)	Averaged X^2 values For LY measurements	Averaged X^2 values For C6 measurements	Averaged X^2 values For C153 measurements	Averaged X^2 values For DPOPOP Measurements
0.622	0.803	1.127	0.930	0.903
0.400	0.817	1.205	0.733	1.267
0.260	0.870	1.227	0.887	1.157
0.165	0.550	1.020	1.247	1.327
0.100	1.287	0.757	0.833	1.320

Table 8: Averaged X^2 values of different fluorophores measured using CCVJ as a reference lifetime standard . Both sample and reference were excited by 405nm laser diode.

CCVJ fluorescence lifetime in 5 different viscosities (nsec)	Averaged X^2 values For LY measurements	Averaged X^2 values For C6 measurements	Averaged X^2 values For C153 Measurements
0.622	0.603	1.567	1.303
0.400	1.080	1.317	1.223
0.260	0.673	1.220	0.957
0.165	0.683	1.620	0.880
0.100	0.817	1.133	0.777

Table 9: Averaged X^2 values of different fluorophores measured using CCVJ as a reference lifetime standard. Both sample and reference were excited by 440nm laser diode.

CCVJ was successfully employed as a reference lifetime standard at 405 and 440nm. The obtained fluorescence lifetimes agreed with the known fluorescence lifetimes of the measured fluorophores (4% variation at the most extreme case) and the X^2 values were around unity. The measured fluorescence lifetime was independent of the standard that was used (Figures 33, 34). This demonstrates that CCVJ can be used as a tunable picosecond reference lifetime standard.

CHAPTER 8

Discussion

8.1 Viscosity and fluorescence lifetime model

CCVJ's intensity was previously used for blood plasma viscosity determination (Haidekker and others 2002). However, errors arising from concentration inaccuracies affected those measurements. In order to eliminate these errors, this research project employed time resolved spectroscopy. The intensity and fluorescence lifetime were measured for 5, 7 and 10 Micro molar CCVJ in glycerol (Figures 25, 26). Increasing the probe's concentration caused a large intensity increase of 0.56 million counts per second (about 50% increase) between the 5 and 10 Micro molar concentrations. However, the fluorescence lifetime showed only a slight variation of 18 picoseconds (about 3% variation) between the 5 and 10 Micro molar concentrations. This decrease in fluorescence lifetime is attributed to inner filter effects and so it is recommended to work with CCVJ concentrations below 10 Micro molars.

Forster and Hoffmann (1971) described the intensity dependency on viscosity of fluorescent molecules that undergo TICT formation using a power law relationship (Forster and Hoffmann 1971). For the fluorescence lifetime and viscosity model the same approach was taken and the R^2 values agreed with this approach. The intensity viscosity model that was obtained was described by $I=0.01093*\eta^{0.5917}$ with $R^2=0.9949$ (Figure 27). in this case, X= 0.5917 is in perfect agreement with Forster and Hoffmann (1971) X=0.6. However, when looking at the fluorescence lifetime viscosity models that were obtained:

$\tau=0.01684*\eta^{O.5302}$ where $R^2=0.9956$ (DPOPOP as reference lifetime) and $\tau=0.02022*\eta^{O.4988}$ where $R^2=0.9932$ (CCVJ as reference lifetime) in both cases X decreases (Figures 28, 29). Since more information was used in constructing the second model where CCVJ was used as a reference lifetime (10-300Mhz compared to 10-200Mhz when DPOPOP was used as a reference), this model was chosen as better representation of the fluorescence lifetime viscosity dependency. X in this case, approximately equals 0.5 rather than 0.6 as in the intensity viscosity model. I think we can accept that since Forster and Hoffmann (1971) provided their X=0.6 for and concluded that X is a dye-dependent constant (Forster and Hoffmann 1971).

CCVJ exhibited a single exponential decay in all of the measurements. This result is supported by Iwaki and others (1993) who also found CCVJ to have a single exponential decay(Iwaki and others 1993). The fluorescence lifetimes were measured using DPOPOP and CCVJ as reference lifetimes. The results obtained showed great similarity (Table 3) however; the fluorescence lifetimes that were obtained when CCVJ was used as a reference lifetime were used in describing the fluorescence lifetime viscosity model and when establishing CCVJ as reference lifetime standard (again for the same reason that more information could be obtained). The viscosity range was between 945 and 13.35 mPa*s corresponding to lifetimes between 0.619 and 0.098 nanoseconds, respectively (Table 3).

A correlation between the fluorescence lifetime and emission intensity showed a significant linear fit $R^2=0.9927$ (Figure 30). This linear correlation

supports the hypothesis that CCVJ's fluorescent lifetimes may be used to determine viscosities.

We hypothesis that at lower viscosities CCVJ would yield lower fluorescence lifetimes. However, we were limited by our device and weren't able to accomplish these measurements. A frequency domain device that uses a MCP for detection may help resolve the low viscosities due to the high frequency response (GHz) and short transit time spreads of MCP's. However, the additional cost of $35K is very high.

8.2 CCVJ's fluorescence lifetime as a viscosity measurement tool

CCVJ shows a great promise as an alternative approach for viscosity measurements. Its microviscosity sensitivity maybe exploited for cellular viscosity measurements and the fluorescent lifetime viscosity model can be used to determine cellular components viscosity. The pharmaceutical industry could use CCVJ's fluorescence lifetime to monitor viscosity changes due to drug effects. Again the fluorescent lifetime viscosity model can be used to determine the actual viscosity rather than trends. For blood plasma anomalies detection, viscosities between 1.5mPa*s and 5mPa*s must be measured. In this research, we were limited by our device and were not able to measure the fluorescence lifetimes at those viscosities. As mentioned before, a 1GHz phase modulation spectrometer could help modeling the lower viscosities.

Measurement time is an important factor for viscosity measurements. Our initial measurements took between 5 and 7 minutes which is far too long for

clinical applications. In order to reduce the measurement time we exploited the fact that CCVJ exhibits a single exponential decay and so the fluorescence lifetime can be determined using only a few data points. Phase modulation data at 10, 40, and 120MHz was successfully used to determine CCVJ's fluorescence lifetime reducing the measurement time to 30 seconds (Table 4). Both sample size and preparation time for sequential measurements can be reduced by using disposable micro-cuvettes. These micro-cuvettes are available from OCEAN OPTICS and can hold samples as low as 70 Micro liters.

8.3 CCVJ as a tunable picoseconds fluorescence lifetime standard

One of the challenges encountered during this research was to find a suitable reference lifetime standard. DPOPOP with fluorescent lifetime of 1.45nsec worked well at frequencies bellow 200MHz, but a picoseconds reference lifetime standard would make it possible to use an even higher modulation frequency which would yield more information about CCVJ's behavior. Since CCVJ exhibited a single exponential decay it was suggested that it can be used as a reference lifetime standard. The fluorescent lifetimes obtained using CCVJ as reference lifetime standard were very close to the ones obtained when DPOPOP was used (Table 4). However, phase modulation measurements were obtained at 300MHz increasing the amount of information by 50%. In some cases, it was even possible to obtain measurements at 400 and 450MHz with good X^2 values (Figure 31). For CCVJ to be considered as a reference lifetime standard it has to exhibit several characteristics.

1) It has to exhibit single exponential decay which it did in all of our measurements.
2) The fluorescent lifetime should be independent of excitation wavelength. Two excitation light sources of 405nm and 440nm were used to validate this criterion. The results showed only a very small change in fluorescence lifetimes which are probably due to mixing and machine inaccuracies (Table 7).
3) The fluorescence lifetime must be short (around 1ns) in order to avoid oxygen quenching. The fluorescent lifetimes for CCVJ in range of frequencies of 945 to 13.35 mPa*s were found to be 0.618 to 0.098 nanoseconds respectively, satisfied this requirement.
4) A large stoke shift is recommended to reduce overlapping of absorption and emission spectra. CCVJ's in glycerol exhibits a Stoke's shift of 53nm where ideal absorption occurs at 437nm and ideal emission peaks at 490nm (Figure 24).
5) It is recommended that the reference lifetime standard would be commercially available. This is true in the case of CCVJ which was purchased at Sigma-Aldrich.

CCVJ was tested and successfully satisfied all of the criteria mentioned above but in order to provide an even stronger validation for the use of CCVJ as a reference lifetime standard we performed an additional experiment. Four different fluorophores with known fluorescent lifetimes and similar excitation emission wavelengths to CCVJ (except from DPOPOP which cannot be excited at 440nm)

were chosen. These dyes were measured using CCVJ in 5 different viscosities as reference lifetime Standards using both 405nmand 440nm laser diodes as excitation sources (Figures 33, 34). The measured lifetimes showed only a small difference from the known lifetimes (4% in the most extreme case) while the X^2 values where around unity (Tables 8, 9). The linear fit showed no significant deviation from zero which shows that the measured fluorescence lifetime was independent of the standard that was used (Figures 33, 34). These results helped validate CCVJ as a tunable picoseconds reference lifetime standard.

CCVJ is the first tunable picoseconds reference lifetime standard. Its unique fluorescence lifetime viscosity dependency can be used to change its fluorescence lifetime and tailor it one's needs. We have shown the fluorescence lifetimes between 945 and 13.35 mPa*s to be between 0.610 and 0.098 nanoseconds, respectively. However, a shorter fluorescent lifetime might be achieved in solvents of lower viscosities.

CHAPTER 9

Conclusions

The fluorescence lifetime viscosity dependency of CCVJ can be used as an alternative approach for viscosity measurements which currently rely on mechanical principles. Using fluorescence lifetime rather than intensity measurements eliminates errors arising from concentration inaccuracies and might allow for simultaneous measurements of several cellular components. The fluorescence lifetime viscosity model described in this thesis will help future researchers determine the viscosities of their studied environments.

The second objective of this research was to supply a picoseconds reference lifetime standard which can be excited with wavelengths between 400 and 460nm. CCVJ was shown to behave as a reference lifetime standard at this wavelength range and its fluorescent lifetime showed a tunable range of 0.618 to 0.098 nanoseconds.

REFERENCES

1. Akers WJ, Cupps JM, Haidekker MA. 2005. Interaction of fluorescent molecular rotors with blood plasma proteins. Biorheology, 42(5):335-344.

2. Anonymous. 1984. Recommendation for a selected method for the measurement of plasma viscosity. International Committee for Standardization in Haematology. J Clin Pathol, 37:1147-1152.

3. Badugu R, Lakowicz JR, Geddes CD. 2005. Fluorescence sensors for monosaccharides based on the 6-methylquinolinium nucleus and boronic acid moiety: potential application to ophthalmic diagnostics. Talanta, 65(3):762-768.

4. Bambot SB, Rao G, Romauld M, Carter GM, Sipior J, Terpetchnig E, Lakowicz JR. 1995. Sensing oxygen through skin using a red diode laser and fluorescence lifetimes. Biosensors and Bioelectronics, 10(6-7):643-652.

5. Barrow DA, Lentz BR. 1983. The use of isochronal reference standards in phase and modulation fluorescence lifetime measurements. J. Biochem. Biophys. Methods, 7(3):217-234.

6. Boens N, Qin W, Basaric N, Hofkens J, Ameloot M, Pouget J, Lefevre JP, Valeur B, Gratton E, vandeVen M, Silva ND, Jr., Engelborghs Y, Willaert K, Sillen A, Rumbles G, Phillips D, Visser AJ, van HA, Lakowicz JR, Malak H, Gryczynski I, Szabo AG, Krajcarski DT, Tamai N, Miura A. 2007. Fluorescence lifetime standards for time and frequency domain fluorescence spectroscopy. Anal. Chem., 79(5):2137-2149.

7. Carreon JR, Stewart KM, Mahon J, Shin S, Kelley SO. 2007. Cyanine dye conjugates as probes for live cell imaging. Bioorganic & Medicinal Chemistry Letters, 17(18):5182-5185.

8. Chakraborty A, Basak S. 2007 pH-induced structural transitions of caseins. Journal of Photochemistry and Photobiology B: Biology, 87(3):191-199.

9. Cinar Y, Senyol AM, Duman K. 2001. Blood viscosity and blood pressure: role of temperature and hyperglycemia. American Journal of Hypertension, 14(5):433-438.

10. Cokelet GR. 1972. The rheology of human blood, in: Biomechanics: Its Foundations and Objectives, Englewood Cliffs, NJ: Prentice-Hall. p 63-103.

11. Doolittle AK. 1952. Studies in Newtonian Flow. III. The Dependence of the Viscosity of Liquids on Molecule Weight and Free Space (in Homologous Series). J. Appl. Physiol, 23:236-239.

12. Douglas M, Roger W, Paul GS. 2002. Fluorescence Quantum Yields and Their Relation to Lifetimes of Rhodamine 6G and Fluorescein in Nine Solvents: Improved Absolute Standards for Quantum Yields. Photochemistry and Photobiology, 75(4):327-334.

13. Fantini S, Franceschini MA, Fishkin JB, Barbieri B, Gratton E. 1994. Quantitative determination of the absorption spectra of chromophores in strongly scattering media: light emitting-diode-based technique. Appl.Opt, 33:5204-5213.

14. Forster T, Hoffmann G. 1971 Die Fluoreszenzausbeuten einiger Farbstoffsysteme (The fluorescence yield of some dye systems). ZPhys Chem 75:63-76.

15. Gaviola Z. 1926. Ein Fluorometer, apparat zur messung von fluoreszenzabklingungszeiten. Z Phys, 42:853-861.

16. Geddes CD, Apperson K, Karolin J, Birch DJS. 2001. Chloride-Sensitive Fluorescent Indicators. Analytical Biochemistry, 293(1):60-66.

17. Grabowski ZR, Grellmann KH, Rotkiewicz K. 1973. Reinterpretation of the anomalous fluorescense of p-n,n-dimethylamino-benzonitrile. Chemical Physics Letters, 19(3):315-318.

18. Haidekker MA, Tsai AG, Brady T, Stevens HY, Frangos JA, Theodorakis E, Intaglietta M. 2002. A novel approach to blood plasma viscosity measurement using fluorescent molecular rotors. Am. J. Physiol Heart Circ. Physiol, 282(5):H1609-H1614.

19. Haidekker MA, Ling T, Anglo M, Stevens HY, Frangos JA, Theodorakis EA. 2001. New fluorescent probes for the measurement of cell membrane viscosity. Chemistry & Biology, 8(2):123-131.

20. Harkness J. 1971. The Viscosity of Human Blood Plasma; Its Measurement in Health and Disease. Biorheology, 8:171-193.

21. Heilmann L. 1986. [Changes in flow properties of the blood in pregnancy]. Zentralbl. Gynakol., 108(7):393-402.

22. Huber C, Fahnrich K, Krause C, Werner T. 1999. Synthesis and characterization of new chloride-sensitive indicator dyes based on dynamic fluorescence quenching. Journal of Photochemistry and Photobiology A: Chemistry, 128(1-3):111-120.

23. ISS.com Accessed 1-10-2007. Topic: Fluorophores fluorescence lifetime. http://www.iss.com/resources/lifetime.html

24. Iwaki T, Torigoe C, Noji M, Nakanishi M. 1993. Antibodies for fluorescent molecular rotors. Biochemistry, 32(29):7589-7592.

25. Jamieson T, Bakhshi R, Petrova D, Pocock R, Imani M, Seifalian AM. 2007. Biological applications of quantum dots. Biomaterials, 28(31):4717-4732.

26. Kaminov IP. 1984. An introduction to electrooptic devices. New York: Academic Press. 409p.

27. Kaperonis AA, Michelsen CB, Askanazi J, Kinney JM, Chien S. 1988. Effects of total hip replacement and bed rest on blood rheology and red cell metabolism. J. Trauma, 28(4):453-457.

28. Krasnowska EK, Bagatolli LA, Gratton E, Parasassi T. 2001. Surface properties of cholesterol-containing membranes detected by Prodan fluorescence. Biochimica et Biophysica Acta (BBA) - Biomembranes, 1511(2):330-340.

29. Kumari M, Marmot M, Rumley A, Lowe G. 2005. Social, Behavioral, and Metabolic Determinants of Plasma Viscosity in the Whitehall II Study. Annals of Epidemiology, 15(5):398-404.

30. Kung C, Reed J. 1986. Microviscosity measurements of phospholipid bilayers using fluorescent dyes that undergo torsional relaxation. Biochemistry, 25:6114-6121.

31. Kung C, Reed J. 1989. Fluorescent molecular rotors: a new class of probes for tubulin structure and assembly. Biochemistry, 28:6678-6686.

32. Lakowicz JR. 2006. Principles of Fluorescence Spectroscopy. New York: Springer Science+Business Media, LLC. 954p.

33. Lakowicz JR, Cherek H, Balter A. 1981. Correction of timing errors in photomultiplier tubes used in phase-modulation fluorometry. J. Biochem. Biophys. Methods, 5(3):131-146.

34. Lakowicz JR, Gryczynski I, Gabor Laczko, Dieter Gloyna. 1991. Picosescond Fluorescence Lifetime Standards forFrequency- and Time-Domain Fluorescence. J. Fluoresc, 1(2):87-94.

35. Lakowicz JR, Laczko G, Gryczynski I, Szmacinski H, Wiczk W. 1988. New trends in photobiology: Gigahertz frequency-domain fluorometry: Resolution of complex decays, picosecond processes and future developments. Journal of Photochemistry and Photobiology B: Biology, 2(3):295-311.

36. Lei LM, Wu YS, Gan NQ, Song LR. 2004. An ELISA-like time-resolved fluorescence immunoassay for microcystin detection. Clinica Chimica Acta, 348(1-2):177-180.

37. Letcher RL, Chien S, Pickering TG, Sealey JE, Laragh JH. 1981. Direct relationship between blood pressure and blood viscosity in normal and hypertensive subjects. Role of fibrinogen and concentration. Am. J. Med., 70(6):1195-1202.

38. Lippert E, Luder W, Boos H. 1962. Advances in Molecular Spectroscopy. Mangini A, ed. Oxford, England: Pergamon Press. 443 p.

39. Loutfy R. 1986. Fluorescence probes for polymer free-volume. Pure Appl Chem, 58:1239-1248.

40. Mauzerall D, Ho PP, Alfano RR. 1985. The use of short lived fluorescent dyes to correct for artifacts in the measurements of fluorescence lifetimes. Photochem. Photobiol., 42(2):183-186.

41. McGrath MA, Penny R. 1976. Paraproteinemia: blood hyperviscosity and clinical manifestations. J. Clin. Invest, 58(5):1155-1162.

42. McMillan DE. 1982. Further observations on serum viscosity changes in diabetes mellitus. Metabolism, 31(3):274-278.

43. Mishra PP, Koner AL, Datta A. 2004. Interaction of Lucifer yellow with cetyltrimethyl ammonium bromide micelles and the consequent suppression of its non-radiative processes. Chemical Physics Letters, 400(1-3):128-132.

44. Molecular Expressions Accessed 1-10-2007. Topic: Photomultiplier tube http://micro.magnet.fsu.edu/primer/digitalimaging/concepts/photomultipliers.html

45. Otto C, Ritter MM, Richter WO, Minkenberg R, Schwandt P. 2001. Hemorrheologic abnormalities in defined primary dyslipoproteinemias with both high and low atherosclerotic risks. Metabolism, 50(2):166-170.

46. Rayner DM, McKinnon AE, Szabo AG, Hackett PA. 1976. Confidence in Fluorescence Lifetime Determination: A Ratio Correction of the Photomultiplier Time Response Variations with Wavelength. Canadian Journal of Chemistry, 54:3246-3259.

47. Reinhart WH, Danoff SJ, Usami S, Chien S. 1984. Rheologic measurements on small samples with a new capillary viscometer. J. Lab Clin. Med., 104(6):921-931.

48. Roe PF, Harkness J. 1975. Plasma Viscosity in the Elderly. Gerontol.Clin.(Basel), 17:168-172.

49. Rosenson RS, Shott S, Katz R. 2001. Elevated blood viscosity in systemic lupus erythematosus. Seminars in Arthritis and Rheumatism, 31(1):52-57.

50. Rowe-Taitt CA, Golden JP, Feldstein MJ, Cras JJ, Hoffman KE, Ligler FS. 2000. Array biosensor for detection of biohazards. Biosensors and Bioelectronics, 14(10-11):785-794.

51. Spencer RD, Weber G. 1969. Measurement of subnanosecond fluorescence lifetimes with a cross-correlation phase fluorometer. Ann N Y Acad Sci, 158:361-376.

52. Szmacinski H, Chang Q. 2000. Micro- and Sub-nanosecond Lifetime Measurements Using a UV Light Emitting Diode. Appl. Spectroscopy, 54:106-109.

53. Thompson RB, Gratton E. 1988. Phase fluorometric method for determination of standard lifetimes. Anal. Chem, 60(7):670-674.

54. Tolosa L, Szmacinski H, Rao G, Lakowicz JR. 1997. Lifetime-Based Sensing of Glucose Using Energy Transfer with a Long Lifetime Donor. Analytical Biochemistry, 250(1):102-108.

55. vandeVen M, Ameloot M, Valeur B, Boens N. 2005. Pitfalls and their remedies in time-resolved fluorescence spectroscopy and microscopy. J. Fluoresc., 15(3):377-413.

56. Wahl P, Auchet JC, Donzel B. 1974. The wavelength dependence of the response of a pulse fluorometer using the single photoelectron counting method. Rev. Sci. Instrum, 45(1):28-32.

57. Wells R. 1970. Syndromes of Hyperviscosity. N. Engl. J. Med, 283:183-186.

58. Yudkin JS, Kumari M, Humphries SE, Mohamed-Ali V. 2000. Inflammation, obesity, stress and coronary heart disease: is interleukin-6 the link? Atherosclerosis, 148(2):209-214.

59. Zhu L, Stryjewski WJ, Soper SA. 2004. Multiplexed fluorescence detection in microfabricated devices with both time-resolved and spectral-discrimination capabilities using near-infrared fluorescence. Analytical Biochemistry, 330(2):206-218.

60. Zukauskas A, Vitta P, Kurilcik N, Jursenas S, Bakiene E. Characterization of biological materials by frequency-domain fluorescence lifetime measurements using ultraviolet light-emitting diodes. Optical Materials, Forthcoming, Corrected proof.